

**Optimization of 4-Cylinder Spark Ignition Engine for
Fuel Consumption and Vehicle Performance through
Cylinder Deactivation and Forced Induction**

by

Tey Chee Churn

Dissertation submitted in partial fulfilment of
the requirements for the
Bachelor of Engineering (Hons)
(Mechanical Engineering)

JANUARY 2014

Universiti Teknologi PETRONAS
Bandar Seri Iskandar
31750 Tronoh
Perak Darul Ridzuan

CERTIFICATION OF APPROVAL

**Optimization of 4-Cylinder Spark Ignition Engine for
Fuel Consumption and Vehicle Performance through
Cylinder Deactivation and Forced Induction**

by

Tey Chee Churn

A project dissertation submitted to the
Mechanical Engineering Programme
Universiti Teknologi PETRONAS
in partial fulfilment of the requirement for the
BACHELOR OF ENGINEERING (Hons)
(MECHANICAL ENGINEERING)

Approved by,

(Ir. Dr. Masri Bin Baharom)

UNIVERSITI TEKNOLOGI PETRONAS
TRONOH, PERAK

January 2014

CERTIFICATION OF ORIGINALITY

This is to certify that I am responsible for the work submitted in this project, that the original work is my own except as specified in the references and acknowledgements, and that the original work contained herein have not been undertaken or done by unspecified sources or persons.

TEY CHEE CHURN

ABSTRACT

This project is conducted with the main objective of carrying out simulated engine modification concepts to find the best concept that addresses well on two criteria of the automobile industry, which are low fuel consumption and optimum vehicle performance for a city car. The focus of the project is set on gasoline engine, the more widely used engines for cars in Malaysia. For the purpose of analysis and comparison of the modified engine model, the PERODUA Myvi 1.3 SX is made as the benchmark, with the engine being a 1.3L K3-VE four-stroke four-cylinder gasoline engine. In order to achieve fuel consumption reduction, the author upon the guidance of the supervisor, has decided to adopt the cylinder deactivation technology. As to optimize the vehicle performance particularly the speed and acceleration of the car, forced induction systems are seen as the best solution to boost the performance of the engine in terms of power and torque. The period allocated for the project is for two full semesters (7 months), requiring target achievements up from defining objectives, research and data gathering for concepts generation, simulation of concepts up to the results analysis process and finalization of the best concept. From all the research and studies, few feasible mechanisms of cylinder deactivation and forced induction are combined into a few promising concepts. Virtual modeling through CATIA and theoretical computation with the governing equations provide data for software simulation and analysis. In order to select the ultimate concept, GT Power is used to generate simulation results for fuel consumption and performance of the few selected concepts. The best engine modification concept is the 1-cylinder deactivation (piston removal) with the electric supercharging, which is simulated to have the best efficiency and lowest brake specific fuel consumption at the targeted engine speed range. It also fulfills the basic power requirement of 18.2kW and torque of over 89.6Nm. Minor experiments like fuel consumption test and engine vibration test are conducted for validation of simulation data. As the cylinder deactivation concept compromises the balance of the engine cranktrain, balancers are to be mounted on the crankpin of the deactivated cylinders. ADAMS simulation proves the balancers effective as they lower both the unbalance vibration forces and moments.

ACKNOWLEDGEMENT

The author would like to express his utmost gratitude to the **project supervisor Ir. Dr. Masri bin Baharom** and **co-supervisor Mr. Mohd. Syaifuddin Bin Mohd.** for their inspiring supervision and guidance to direct the author from the start till the very end of the project. They have provided supports and technical advises for the author to expand his knowledge on the field of study in theory, practical as well as in industrial standards. On any shortcomings in performance, Ir. Dr. Masri bin Baharom will always give beneficial suggestions on rooms of improvement. Both the supervisors have guided the author throughout the whole project with great enthusiasm and professionalism.

Not forgetting the **lab technician Mr. Muhaimin, Mr. Mahfuz** and **Mr. Firman** for their guidance and assistance in CATIA modeling as well as for the engine familiarization process where the author gets to learn closely about the working principles of the four-cylinder gasoline engine through disassembling and re-assembling of the real engine during lab time. Tutorial on CATIA has proven useful to the author for completion of the modeling of the piston assemblies. Mr. Firman's expertise on GT Power has been a great help to the author regarding complications over the complex engine mappings simulation.

For all the suggestions and critics of the **examiners and evaluators**, utmost gratitude is dedicated for **A.P. Dr. Zainal Ambri Bin Abdul Karim** and **Dr. Varaha Vehkata Lakshmi Narasimha Rao Tad** for their great insights on the project for future improvements.

Deepest appreciation is directed to the **Final Year Project course coordinators, Dr. Masdi Muhammad** and **Dr. Azmi Bin Abdul Wahab** for coordinating the programme effectively, and to make it simple for the author as well as other undergraduates to accomplish their assigned tasks. The briefings conducted by Dr. Masdi have helped to clear all doubts of the author and kept the author on schedule to finish the project.

TABLE OF CONTENTS

CERTIFICATION	i
ABSTRACT	iii
ACKNOWLEDGEMENT	iv
LIST OF FIGURES	vi
LIST OF TABLES	vii
ABBREVIATIONS AND NOMENCLATURES	viii
CHAPTER 1: INTRODUCTION	1
1.1 Project Background	1
1.2 Problem Statement	4
1.3 Objective and Scope of Study	4
CHAPTER 2: LITERATURE REVIEW	5
2.1 Cylinder Deactivation	5
2.2 Forced Induction Devices	9
2.3 Critical Literature Analysis	13
CHAPTER 3: METHODOLOGY	15
3.1 Research Methodology	15
3.2 Project Activities	16
3.3 Key Milestones	21
3.4 Gantt Chart	22
CHAPTER 4: RESULTS AND DISCUSSION	23
4.1 Concept Generation	23
4.2 Data Gathering	24
4.3 GT Power Simulation and Analysis	25
4.4 ADAMS Simulation and Analysis	38
CHAPTER 5: CONCLUSION AND RECOMMENDATION	44
5.1 Conclusion	44
5.2 Recommendations	44
REFERENCES	46
APPENDICES	49

LIST OF FIGURES

Figure 1.1	Power and Torque Curve of K3-VE Engine	3
Figure 2.1	Cylinder Deactivation Technology for Pushrod Designs	7
Figure 2.2	Cylinder Deactivation Technology for Overhead Cam Designs	8
Figure 2.3	Cylinder Deactivation Technology for Camless Designs	8
Figure 2.4	Comparison of the Ideal Dual-Fuel Cycle of a Natural Aspirated Engine and a Supercharged Engine	9
Figure 2.5	Torque vs. Engine Speed Graph for Electric Supercharger-equipped Turbo Engine (VTES)	12
Figure 3.1	Project Methodology	15
Figure 3.2	Arrangement of Crank Throws of the Engine Crankshaft	18
Figure 4.1	GT Power Engine Map of the K3-VE 4-Cylinder Gasoline Engine	25
Figure 4.2	Brake Power Curve of the Actual and Simulated Engine	26
Figure 4.3	Brake Torque Curve of the Actual and Simulated Engine	26
Figure 4.4	Brake Power Curve of Different Cylinder Deactivation Methods	28
Figure 4.5	Brake Torque Curve of Different Cylinder Deactivation Methods	28
Figure 4.6	Total Fuel Consumption Per Cylinder of Different Deactivation Methods	29
Figure 4.7	Total Fuel Consumed by 1.3L Myvi under Different Engine Condition	31
Figure 4.8	BSFC Graph of Different Cylinder Deactivation Methods	31
Figure 4.9	Brake Efficiency of Different Cylinder Deactivation Methods	32
Figure 4.10	Brake Power Curve of Different Combinations	33
Figure 4.11	Brake Torque Curve of Different Combinations	34
Figure 4.12	Total Fuel Consumption of Different Combinations	35
Figure 4.13	BSFC of Different Combinations	35
Figure 4.14	Brake Efficiency of Different Combinations	36

Figure 4.15	ADAMS View of Cylinder Deactivation and Balancing	40
Figure 4.16	Resultant Magnitude of Vibration of Crankshaft of the Normal Engine	41
Figure 4.17	Magnitude of Vibration of Crankshaft with 2 Deactivated Cylinders	41
Figure 4.18	Vibration of Crankshaft with Balancers for Cylinder Deactivation	42
Figure 4.19	Resultant Moment of Crankshaft (Without Steel Balancer)	43
Figure 4.20	Resultant Moment of Crankshaft (With Steel Balancer)	43

LIST OF TABLES

Table 1.1	Engine Specification for a PERODUA Myvi	3
Table 3.1	Key Milestones	18
Table 4.1	Engine Parameter Values Acquired Online	24
Table 4.2	Percentage of Error of Simulated Data	27
Table 4.3	Fuel Consumption of Car over Driving Course of 27.7km	30
Table 4.4	Average Engine Speed for UDDS and HWFET using Different Gears	37
Table 4.5	Tabulated Results of Vibration Test	38
Table 4.6	Tabulated Results of Vibration Amplitude in ADAMS Simulation	42

ABBREVIATIONS AND NOMENCLATURES

ADAMS	– Automated Dynamic Analysis of Mechanical Systems
BMEP	– Brake Mean Effective Pressure
CATIA	– Computer Aided Three-dimensional Interactive Application
CC	– Cubic Centimetres
CMM	– Coordinate-Measuring Machine
DOHC	– Dual Over Head Cam
DVVT	– Dynamic Variable Valve Timing
ECU	– Engine Control Unit
GM	– General Motors Company
ICE	– Internal Combustion Engine
IMEP	– Indicated Mean Effective Pressure
NEDC	– New European Driving Cycle
PEC 2013	– PERODUA Eco-Challenge 2013
PERODUA	– Perusahaan Otomobil Kedua Sendirian Berhad
PETRONAS	– Petroliam Nasional Berhad
SI	– Spark Ignition
TDC	– Top Dead Center
EPA	– Environmental Protection Agency
UDDS	– Urban Dynamometer Driving Schedule
HWFET	– Highway Fuel Economy Test Cycle
BSFC	– Brake Specific Fuel Consumption

CHAPTER 1

INTRODUCTION

1.1 Project Background

The project is selected by the supervisor based on his involvement in the PERODUA Eco-Challenge, a car modification competition for the university. It is actually related to one of the main propositions of the Universiti Teknologi PETRONAS team to compete for the PERODUA Eco-Challenge 2013 (PEC 2013). PEC 2013 challenges all the participating university undergraduates and lecturers on five different aspects: Long Distance, Time Attack, Styling, Engineering and Marketing Challenge to emerge as the Overall Champion [1]. Synchronizing with the competition requirements, the project requires the author to address two main criteria of the automobile industry which are fuel consumption and vehicle performance. The focus of the project is on the city car rather than sports car or heavy duty vehicles. Hence the engine performance has to fulfill the requirement of such categories of cars.

Fuel consumption and carbon dioxide emission reduction have been the two major concerns for the automotive industry for what seems like an eternity. Among the technologies that emerge are active aerodynamics, cylinder deactivation, idle-stop systems, gear shift point display, electric motor-powered cars, regenerative braking etc. Cylinder deactivation has been unanimously agreed upon by the UTP team as the solution to feature for fuel consumption reduction in the PEC 2013. Cylinder deactivation has come into focus of the world in the 80's when it is first featured in the Cardillac's 1981 Seville with the main aim to reduce fuel consumption [2]. This concept revolves around the finding that the typical engine load during daily traffic is low which results in sub-optimal fuel consumption and by applying cylinder deactivation, better

matching of the real engine load with the optimal engine load can be achieved [3]. As a result, the load of the still activated cylinder is increased with improved efficiency [3].

Cylinder deactivation can be adopted in several different methods though. In this project, instead of the typical valve timing technology which is used for relatively bigger engine with more cylinders, a different approach is adopted by removing completely the piston assemblies of the deactivated cylinders as to remove the unnecessary frictional forces between the deactivated pistons with the cylinder wall. This method will affect important criteria regarding the powertrain comfort like engine shake, vehicle shuffle as well as gear rattle as there is a build-up of forces imbalance due to mass reduction [3]. Hence, engine vibrations have to be suppressed, damped or cancelled out.

Vehicle performance has reached such a high point where acceleration and speed of the vehicle achieved is more than required in our daily driving. However, it comes with limitations such as high fuel consumption, big size engine for higher compression ratio, and higher cost. In order to break the frontier of the limitations, optimization of vehicle performance is therefore done in a different approach by downsizing the engine while attaining the energy output. One way of doing it will be to artificially make a smaller engine to breathe in air as if it were larger than it really is [4]. Forced induction techniques such as the conventional turbocharging and supercharging do just that – by force inducting air intake of higher density into the engine to increase the volumetric efficiency. There has been a new product - electric supercharger which is powered up by electricity rather than through the chain connection to the crankshaft of the engine.

Superchargers and turbochargers have long been utilized by mankind in the field of automotives and it can be traced back to the late 1800's where Gottlieb Daimler filed forced induction patent in Germany by supercharging an internal combustion engine [4]. Slightly different from the superchargers, turbochargers are devices that couple a compressor with a turbine driven by the exhaust gases, in order to have the pressure increase proportional to the engine speed [5]. Turbocharger increases the overall system efficiency as more energy is converted from the blowdown of the exhaust gas to provide the compression work of the inlet air.

This project deals specifically with the car engine itself hence the engine specifications are crucial data. The engine selected for benchmarking is the Myvi SX 1.3L (manual transmission). The specification of the engine is outlined in Table 1.1 and Figure 1.1.

TABLE 1.1: Engine Specification for a PERODUA Myvi [6]

Engine Specification	Description
Engine Classification	Four-Stroke Gasoline (SI) Engine
Engine Type	K3-VE
Valve Mechanism	DOHC, 16V with DVVT
Total Displacement	1298 cc
Bore x Stroke	72.0 mm x 79.7 mm
No. of Cylinders	4
Compression Ratio	10.0 : 1
Maximum Output (DIN)	67/6000 kW/rpm
Maximum Torque (DIN)	117/4400 Nm/rpm
Fuel System	Electronic Fuel Injection (EFI)
Fuel Tank Capacity	40.0 L
Transmission	5MT (SX)

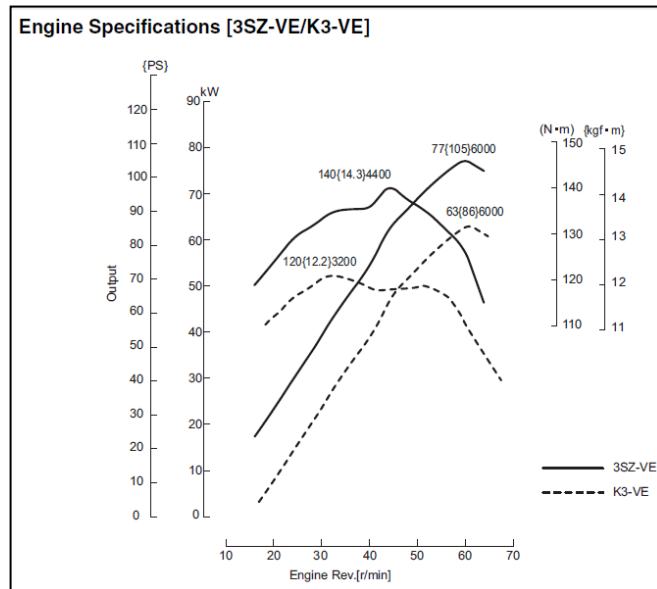


FIGURE 1.1: Power and Torque Curve of K3-VE Engine [7]

1.2 Problem Statements

Based on the requirement of the project, two crucial criteria have to be fulfilled, which are fuel consumption reduction as well as vehicle performance optimization. While there is no restriction to the modification of the engine allowed, there are limitations of financial resources, time, skills and equipments of the UTP team.

1.3 Objective and Scope of Study

The objective of this project is twofold:

1. To reduce fuel consumption of engine by incorporating appropriate cylinder deactivation technology to the simulation model of a 1.3L four-cylinder engine;
2. To maximize the vehicle performance of the car by incorporating a suitable forced induction device to the simulation model;

The scope of study for cylinder deactivation will be the determination of the suitable cylinder deactivation technology to adopt for a city car, the optimal number of pistons to be deactivated as well as the influence of the cylinder deactivation on a four-cylinder engine regarding the dynamic and vibrational behavior of the engine. Balancers of certain weight and size can be employed to dampen or cancel out the resultant imbalance of forces in the engine.

As for the forced induction devices, the scope of study covers all the engine specific parameters required for the adoption of forced induction devices to maximize the vehicle performance while managing their limitations such as eliminating knocking and turbo lag for turbochargers. Software and simulation programs enable virtual modeling, simulations and analysis. The best design parameters will be determined.

CHAPTER 2

LITERATURE REVIEW

2.1 Cylinder Deactivation

For decades, cylinder deactivation has always been deemed one of the most promising technology for reducing emissions and fuel consumption of automobiles. Relentless efforts have been put into research and development which is seen through the first mass production attempt of engines with cylinder deactivation by GM with their Cadillac Eldorado in 1981. However due to certain electronic complications, the technology was used for only one model year before it went out of production [3]. More recently, along with the arising global issue on the fuel crisis as well as environmental concerns, many car manufacturers have returned to this technology to regain advantage over their competitors in the automotive industry. DaimlerChrysler, Honda, Volkswagen, Audi and Mercedes-Benz have all joined the race to put the technology into perfection.

Cylinder deactivation technology aims to reduce fuel consumption as well as emissions of an internal combustion engine during light load operation. The typical power demand for the engine during normal everyday driving is low, supported by the findings that the average power demand of the New European Driving Cycle (NEDC) is 5kW [3]. Due to this low power demand, internal combustion engines operate at low engine load most of the time. During light or low load condition, when the throttle valve is nearly closed, the engine is literally starving for air. The partial vacuum results in higher pumping loss. Engines with large displacement are throttled back so far during light load that the cylinder pressure at top dead center (TDC) can diminish as much as 50% which means low brake mean effective pressure (BMEP) [8]. The efficiency of combustion engines

depends on the engine load and is at its best at high BMEP. Thus, low cylinder pressure leads to low fuel efficiency.

Cylinder deactivation provides solution by combining those two desired operating conditions, which is to achieve high engine BMEP during low power demand. Theoretically, cylinder deactivation requires the remaining active cylinders to operate at higher indicated mean effective pressure (IMEP) to provide the same overall BMEP. BMEP is an indication of the overall engine performance, whereas IMEP is an indication of individual cylinder performance [3]. The use of cylinder deactivation at light load means there are fewer cylinders drawing air from the intake manifold, which works to increase its fluid air pressure. This increases pressure in each operating cylinder and reduces pumping losses. In highway conditions, fuel consumption can be reduced by approximately 20% [8].

Generally, cylinder deactivation is realized by deactivating the valves and blocking injector or ignition signals [3]. Thus, the working principle of cylinder deactivation in variable displacement engines is by simply keeping the intake and exhaust valves for the deactivated cylinders closed through all cycles [9]. There are several industrial-proven mechanisms, depending on design of the engine valve actuation system. Each of the cylinder deactivation technology is given different names, for example the Mercedes-Benz's Active Cylinder Control, Mitsubishi's Modular Displacement, DaimlerChrysler's Multiple Displacement System, GM's Active Fuel Management and Honda's Variable Cylinder Management.

❖ Pushrod Designs

For pushrod designs, collapsible solenoid-controlled valve lifters are installed. The lifters have a spring-loaded locking pin actuated by oil pressure. When cylinder deactivation system is activated, the solenoid system is activated, discharging oil to the reservoir hence the lifter will remain in the position since the oil pressure necessary to push it is removed, hence the valves cannot be actuated and remain closed through all cycles until cylinder deactivation is deactivated [8].

Another type of cylinder deactivation has collapsible valve lifters installed where the lifters have a spring-loaded locking pin which is actuated by oil pressure. The activation mode causes the solenoids to increase the oil pressure and thereby dislodging the locking. As a consequence, the lifter collapses as it is no longer in contact with the pushrod. When the car needs more power, the oil pressure was removed and the lifters are locked back into their full-length configuration [10]. Figure 2.1 shows the basic idea of the processes.

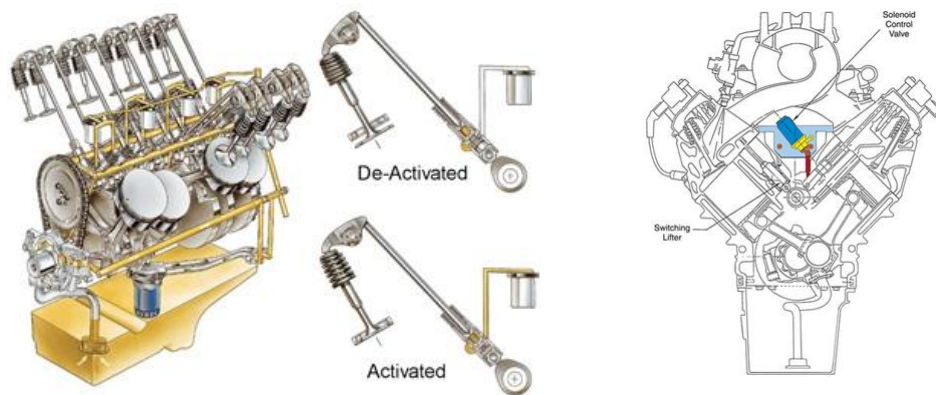


FIGURE 2.1: Cylinder Deactivation Technology for Pushrod Designs [8, 10]

❖ Overhead Cam Designs

For overhead cam designs, a pair of rocker arms which are interlocked is employed for each valve. One rocker follows the cam profile while the other actuates the valve. When cylinder deactivation is employed, solenoid controlled oil pressure releases a locking pin between the two rocker arms. The two rocker arms are no longer in locked together and hence while one arm still follows the camshaft, the unlocked arm remains motionless and the valve remains closed [9].

Another cylinder deactivation technology for overhead cam design engines is adopted by Volkswagen in their new 1.4 TSI gasoline direct injection turbo engine (zylinderabschaltung) [11]. The technology involves electromechanical actuators engaging zero-lift cams via pins and milled guide slots. When the cylinder is

deactivated, the pin will drop into the milled guide slots, turning the movable part of the camshaft inwards or outwards, detaching the valve from the cam profile, hence closing the valves until the pin is lifted. The process is illustrated in Figure 2.2.

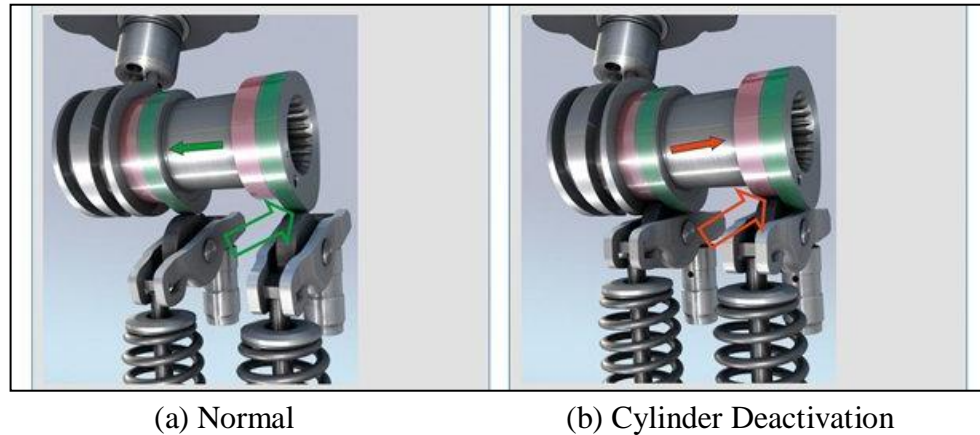


FIGURE 2.2: Cylinder Deactivation Technology for Overhead Cam Designs [12]

❖ Cam-less Designs

The cam-less actuated valves are termed the Valeo system where it uses electromagnetic actuation instead of a mechanical valvetrain [13]. With the valves set default to a partially open position using a pair of springs, a pair of electromagnets is mounted above the valve assemblies with an armature in between. The armature is moved by the electromagnetic fields to actuate the valve. The upper electromagnet pulls the valve shut, and the lower electromagnet pulls to fully open the valve as illustrated in Figure 2.3. Cylinder deactivation can be activated easily through ECU.

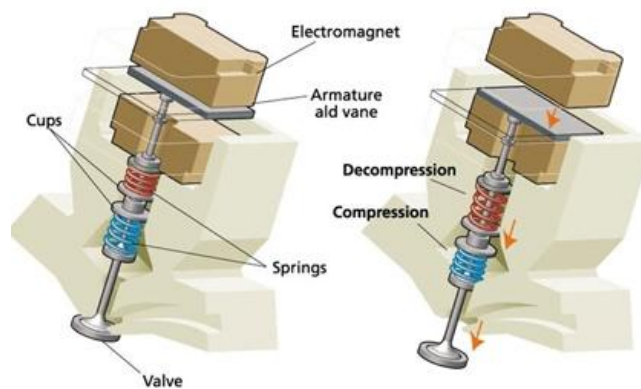


FIGURE 2.3: Cylinder Deactivation Technology for Camless Designs [13]

2.2 Forced Induction Devices

The power of an ICE can be increased through forced induction using an air compression device such as supercharger or turbocharger [14]. Although engine power is generally indicated by its cubic centimetres (cc), a term which portrays the engine displacement (volume), it is the density of the air-fuel mixture or more specifically the mass of fuel and air molecules entering the engine that determine the resultant engine power. The working mechanism is by elevating the pressure and density of the inlet air to allow additional fuel to be injected into the cylinder, subsequently increasing the power produced by each cylinder. Although part of the power output will be consumed in compressing the air for supercharging, the net power output is deemed to be higher than the power output of an engine of the same capacity but without supercharging [15].

2.2.1 Thermodynamic Analysis of Supercharging

The thermodynamic analysis of the supercharged engine cycle can be summarized in Figure 2.4 (b) where Process 8 → 1 is Induction, Process 1 → 2 is Compression, Process 2 → 3 → 4 is Heat Addition, Process 4 → 5 is Expansion, Process 5 → 6 is Heat Rejection, Process 6 → 7 is Exhaust, Process 7 → 8 is Supercharging.

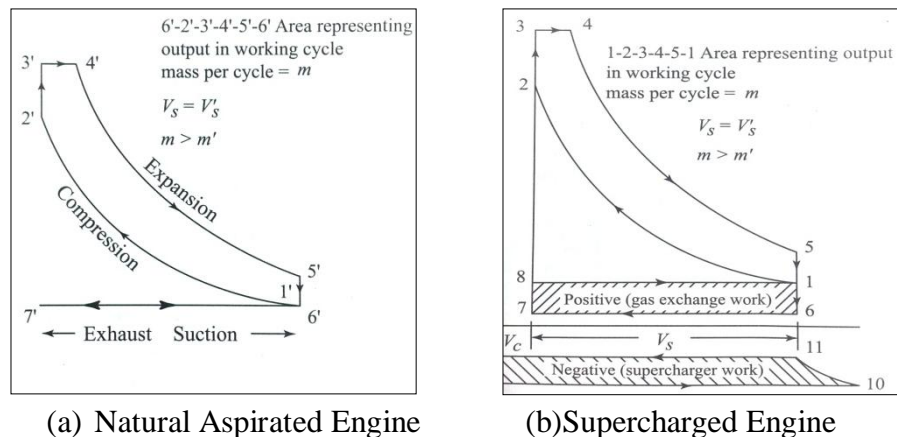


FIGURE 2.4: Comparison of the Ideal Dual-Fuel Cycle of a Natural Aspirated Engine and a Supercharged Engine [15]

Pressure at 6 would be the atmospheric pressure while pressure at 8 will be the elevated pressure of the supercharged air intake. The increase in pressure results in the positive work output which increases the power output for the engine. The positive gas exchange

area 8-1-6-7-8 may be greater than the negative supercharger work of area 9-10-11-12-9 but it indicates that there is a clear loss in work.

Among the crucial limitations for supercharging or turbocharging is the increase in the detonation tendency. As compared to diesel engines, spark ignition engines are knock limited and hence restricting the allowable compressor pressure increase [14]. In many cases, the compression ratio of a SI engine is reduced to mitigate knock when an air compressor is used. As for turbocharger in particular, turbo lag is a common drawback.

2.2.2 Limitations of Turbocharging

One of the limitations of turbocharging is knocking. Knock is a term used to describe the pinging noise emitted from homogenous charge, SI engines [14]. It is more commonly referred as abnormal combustion or knocking combustion which is caused by auto ignition of the unburned or end gas ahead of the flame, creating pressure waves that travel through the combustion gases. It may cause loss of power, recurring pre-ignition and mechanical damage to the engine, thereby need to be avoided [14]. Knocking can be reduced or avoided through regulation of the following few factors [15]:

- ❖ Compression ratio: High compression ratio of engine results in high pressure and temperature of the unburned air-fuel mixture at the end of the compression stroke. The temperature might increase to the extent that it exceeds the auto ignition temperature of the mixture and results in knocking.
- ❖ Mass of Inducted Charge: A reduction in mass of the inducted charge or air-fuel mixture into the cylinder will result in a decrease in both temperature and density of the charge at the time of ignition, hence lowers the tendency of knocking.
- ❖ Inlet Temperature of Mixture: An increase in inlet temperature of the mixture rises the compression temperature as well thereby increasing the tendency of knocking.

- ❖ Air-Fuel Ratio: The air-fuel ratio affects the reaction time of the mixture. The maximum tendency to knock takes place for air-fuel ratio which gives the minimum reaction time.
- ❖ Octane Value of the Fuel: The higher the octane value of the fuel, the higher the compression that the fuel can withstand due to their higher self-ignition temperature and a low pre-flame reactivity thereby reducing the tendency of knocking.

Other less significant factors comprise temperature of the combustion chamber walls, the power output of engine, retardation of the spark timing, location of spark plug, engine size, engine speed, flame travel distance, combustion chamber shape etc.

Another limitation of turbocharging is the turbo lag occurs with a sudden throttle change. When the accelerator pedal is pressed on, throttle is opened quickly, but the turbocharger needs to take several engine revolutions for the exhaust flow rate to increase to speed up the rotor of the turbine to provide the power boost. Thus turbocharger has a lag in respond time as compared to supercharger. The fundamental problem is to get a sufficient volume of exhaust gas to the rotor of the turbine as fast as possible after the throttle is opened wide. Turbo lag can be reduced by using lightweight ceramic rotors to minimize the rotational inertia so it can respond faster to the change in speed [16]. Another alternative is to have a smaller intake manifold. Some manufacturers come out with the anti-lag system and also the twin-turbo. The anti-lag system employs slightly-opened throttle or extra air injector, coupled with ignition delay. Air-fuel mixture will flow into the cylinder after the power stroke and remain unburned until they come in contact with the high temperature exhaust once the exhaust valve is opened. The resultant micro-explosions thereby spin the turbo, providing adequate pressure for the turbo even if the accelerator pedal is lifted [17]. As for the twin-turbo, cars such as the Porsche 959 and Toyota Supra (last gen) utilize the sequential twin-turbo where during low engine speed, the limited amount of exhaust gas is only directed to drive one turbo

to spool it up faster. When the exhaust flow reaches sufficient amount, the engine management system activates the bypass valve for a switchover to involve the second turbo to maximize the boost pressure [18].

One of the best solutions is to have an electric turbocharger as what Audi has done. In order to solve turbo lag as well as the problem of inadequacy of air to spool the turbocharger up to its operating speed at lower engine speed, Audi is working on a new bi-turbo engine which uses an electrically-driven turbocharger [19]. The system is simpler than the twin-turbo set-ups, mainly dependent on a normally inoperative electric turbocharger. During low speeds or from standstill, the air discharged from the main turbocharger will be re-routed through the electric turbocharger to be pressurized as it is already spinning at high speed using the electrical power provided by the motor or a storage battery [19]. Controlled Power Technologies are working in the same approach with the Variable Torque Enhancement System (VTES) [20]. The graph in Figure 2.5 shows that an electric supercharger or turbocharger can solve the main weakness of turbochargers of providing torque below 3000rpm. The whole concept is an area of field for development of the electric supercharger.

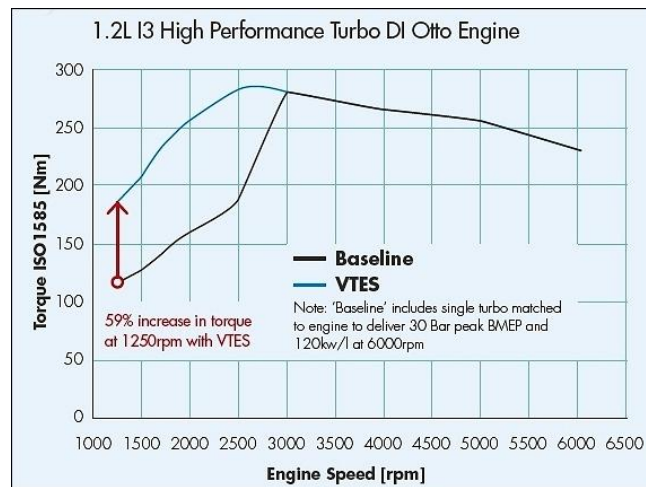


FIGURE 2.5: Torque vs. Engine Speed Graph for Electric Supercharger-equipped Turbo Engine (VTES) [21]

2.3 Critical Literature Analysis

For project-wise, the solutions for problems stated have to be selected based on the ability and limitation of the author. Alternatives those are focus-studied in literature review under sub-chapters 2.1 and 2.2 are evaluated for the finalization of the solution.

Cylinder deactivation lowers the frequency of the combustion torque pulses onto the crankshaft, making the active cylinders operating under higher load in order to maintain the output torque [3]. On the other hand, reduced combustion interval and increased combustion peaks increase the torsional vibrations of the engine [3]. Besides the deactivated pistons will still be reciprocating during cylinder deactivation. Thus the unnecessary frictional forces between the piston and the cylinder wall will degrade the performance of the engine. Some argue that since the valves remain closed throughout the deactivation period, energy is lost through the compression of the dead air by the deactivated pistons which otherwise termed as the pumping loss. However, manufacturers claim that the loss is minimal as there is an almost 100% offset when the compressed air expands and pushes back against the pistons during the down-stroke [22].

Although all the limitations can be eliminated through more advanced cylinder deactivation technology, it requires highly technical and costly modifications with additional actuators and spaces. For instance, an integrated starter alternator damper can be employed to suppress the torsional vibrations due to cylinder deactivation but such a sophisticated damper costs a fortune for its current technology availability [3]. The author does not have the necessary resources, equipments and time for them. Therefore, the solution agreed upon by the supervisor for the cylinder deactivation is to remove two piston assemblies completely and have the valves of the deactivated cylinders deactivated as well in order to prevent pumping loss and frictional forces between the piston and cylinders. The removal of piston assemblies will affect the entire powertrain comfort by causing engine shake and vibrations, eventually compromising the performance of the engine. The unbalance forces and moments developed in the engine have to be suppressed, damped or cancelled out. One way of cancelling out the unbalance forces is to add balancers to the crank pin of the removed pistons to counterweigh the lost in mass of the pistons removed.

Supercharging or turbocharging is a great solution but a perfect balance between power generation and knocking tendency has to be found for vehicle performance optimization. Out of the five major factors contributing to knocking, only a few can be regulated. Although the engine is subjected to modification, it will be difficult to alter the cylinders' compression ratio. The conventional supercharger is torqued by the crankshaft and hence may consume as much as 20% of the engine power [15]. It also puts additional strain to the engine. Electric supercharger can be seen as another new alternative using an external 24V battery to power up the supercharger. No power will be consumed from the engine but from the battery.

CHAPTER 3

METHODOLOGY

3.1 Research Methodology

This project was carried out based on the sequential processes of the methodology from one task to another. There were instances where a step back of process is needed for changes and modification when a certain process cannot be accomplished. Each process is specified with more objective-focused activities in the section of Project Activities and Key Milestones. The sequential processes are summarized in Figure 3.1.

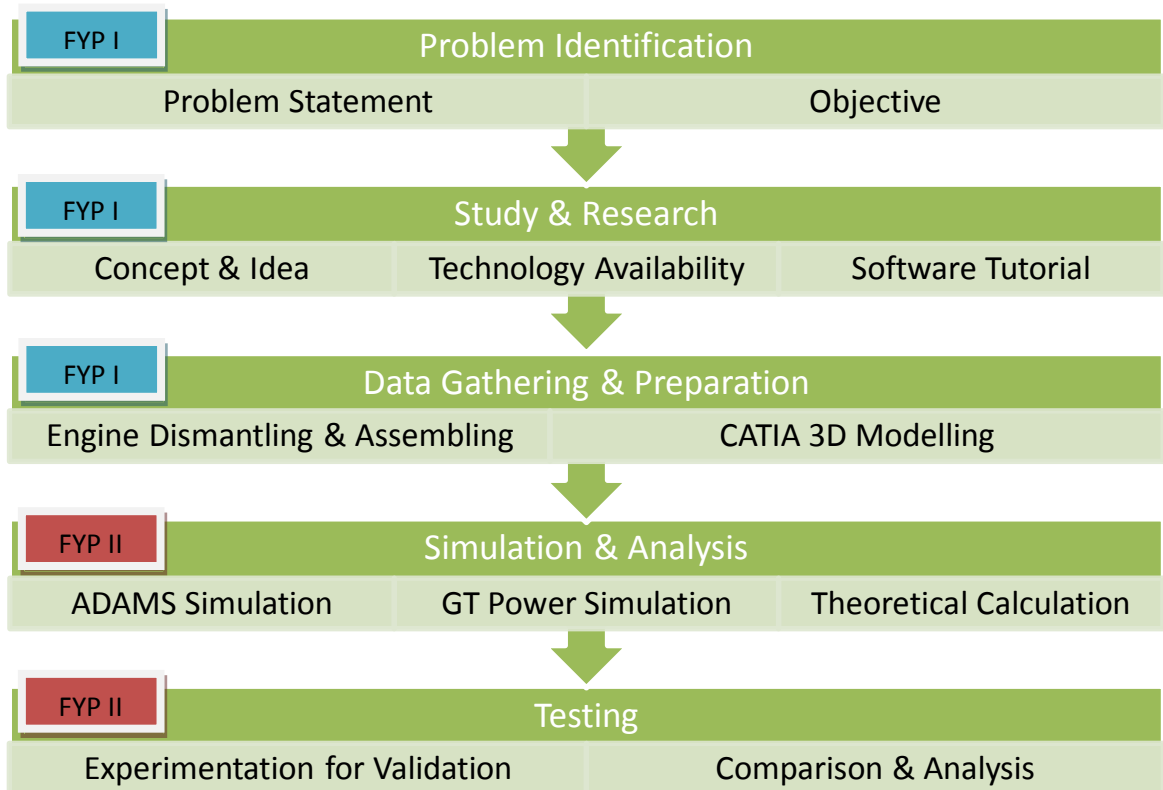


FIGURE 3.1: Project Methodology

3.2 Project Activities

Detailed activities and tasks are listed out for each process of the methodology. The section below pinpoints the different project activities required under different steps.

a) Problem Identification

In order to start the project, the problem statement was determined in order to set the objectives of the project. A consultation was conducted with the supervisor of the project, Ir. Dr. Masri Baharom in order to understand the scope of study on the engine modification. Co-supervisor, Mr. Mohd. Syaifuddin Bin Mohd. was consulted as well before setting the objectives which were built on the problem statement. The scope of the study of the project was set and the title of the project was redefined.

b) Study & Research

Previous related projects information had been acquired from the supervisor for reference to get a basic concept and idea of starting the project. The solution for the problem statement has been scoped down by the supervisor to cylinder deactivation and forced induction so focused study and research were carried out to define different concepts available. Internet researches had been useful to check on the technological availability of the concepts too. The Engine Design lectures had helped to grasp the knowledge and understanding on the engine's working principal and performance analysis. Software tutorial and training were given by the lab technicians in Building 17 on CATIA, ADAMS as well as GT Power.

c) Data Gathering & Preparation

A K3-VE engine overhaul had been carried out in a workshop so actual dimension of the engine was measured accurately to resemble the real components in 3D modeling as well as for the data for GT Power Simulation for effective analysis. Other information has been acquired from the manufacturing sectors through websites and brochures. CATIA was then used to structure the 3D model as the fundamental preparation for ADAMS simulation.

d) Analysis & Simulation

The GT Power engine map of the K3-VE engine was constructed based on the engine parts' dimensions as well as other parameters which were acquired online, measurement or assumptions. The power and torque curve produced by the GT power was compared to the actual K3-VE curve for validation. Modifications were done to the assumptions to assimilate the results as close as possible to the actual curves. Next, modifications were carried out for different cylinder deactivation methods. The required power and torque of the car was computed and set as the standard to benchmark the cylinder deactivation methods. Only few methods were selected and modified with combinations with the forced induction systems. The final simulation results were analyzed based on several outcome parameters, such as brake power, brake torque, brake efficiency, total fuel consumption as well as BSFC.

As for the balancing effort, the 3D model of the piston-crankshaft assembly was imported from CATIA into ADAMS. For kinematic analysis, various types of joint were defined at specific coordination to link different components together to enable relative movements. Main joints included the crank pin connecting the connecting rod with the crankshaft and the gudgeon pin linking the connecting rod to the piston, making sure that the crankshaft rotates accordingly to the reciprocation of the pistons. A force was applied downwards onto the top of each piston to represent the expansion force due to combustion of the mixture of air and fuel. Simulation was run and the results were generated in the form of graphs for analysis.

It is important to know the average engine speed of the car to determine the scope of analysis of the vehicle performance and fuel consumption. The governing equation used for calculating the average engine speed based on average vehicle speed is as the formula 3.1 below.

$$N_p = \frac{30 \cdot V \cdot i_g \cdot i_0}{\pi \cdot r_d} \quad \text{----- (3.1)}$$

where V = vehicle speed; i_g = gear ratio; i_0 = final drive ratio; r_d = effective wheel radius

For the balancing effort, the theories and equations are as follow.

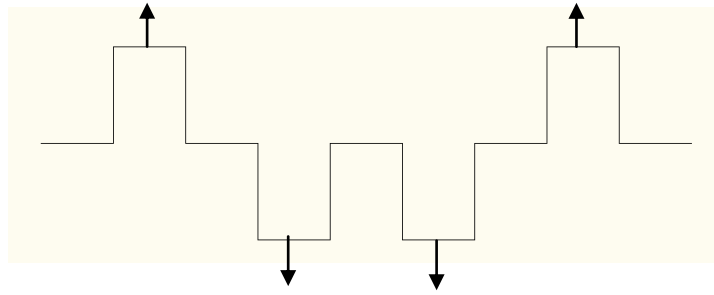


FIGURE 3.2: Arrangement of Crank Throws of the Engine Crankshaft

For multi-cylinder cranktrain balancing, the 4-cylinder K3-VE engine has arrangement of crank throws as in Figure 3.2, resulting in the following free forces and moments;

$$\Sigma F_1 = 0 ; \Sigma F_2 = 4F_2 ; \Sigma M_{F1} = 0 ; \Sigma M_{F2} = 0$$

For two cylinder deactivation, the primary step is to determine the two pistons to be deactivated. The best choice determined is to either deactivate piston 1&3 or piston 2&4, which results in the same dynamics below. Piston 1&3 are selected to be deactivated.

$$\begin{aligned} \Sigma F_1 &= 0 ; \Sigma F_2 = 2F_2 ; \\ \Sigma M_{F1} &= F_1(3a/2) + F_1(a/2) = 2F_1a ; \\ \Sigma M_{F2} &= F_2(3a/2) - F_2(a/2) = F_2a \end{aligned}$$

Consider having two balancers each generating F_x mounted at the crankpin of the deactivated pistons, the equations of the resultant forces and moments are as below

$$\begin{aligned} \Sigma F_1 &= 0 ; \\ \Sigma F_2 &= 2(F_2 + F_x) ; \\ \Sigma M_{F1} &= F_1(3a/2) + F_1(a/2) - F_x(3a/2) + F_x(a/2) = 2a(F_1 - F_x) ; \\ \Sigma M_{F2} &= F_2a \end{aligned}$$

It is seen that with the addition of two balancers, the resultant primary forces ΣF_1 as well as the moment due to the secondary forces ΣM_{F2} will not increase. It is noticed that an increase in F_x will increase F_2 but decreases ΣM_{F1} .

As for single-cylinder mass balancing, between the secondary forces and resultant moment due to primary forces, it is desirable for lower ΣM_{F1} while compromising the engine with higher ΣF_2 because F_2 is usually very small and can be negligible. Hence for optimum balancing, ΣM_{F1} should be as small as possible. Formulas for the forces are;

- Primary forces, $F_1 = m_{osc}r\omega^2 (\cos \alpha)$ ----- (3.2)

- Secondary forces, $F_2 = m_{osc}r\omega^2 (\lambda \cos 2\alpha)$ ----- (3.3)

- Balancer Balancing Forces, $F_x = m_x r \omega^2$ ----- (3.4)

For minimal ΣM_{F1} , F_x should be equal to maximum F_1 .

$$\text{Maximum } F_1 = m_{osc}r\omega^2 = m_x r \omega^2 \text{ ----- (3.5)}$$

Since the angular velocity is constant throughout the crankshaft and the two balancers will be mounted at the same crank radius away from the main journal, m_x should equal to m_{osc} . (**r and ω = constant**)

The calculation of the oscillating masses is as follow;

$$M_{conrod''} = M_{conrod} (l_1/l) \text{ ----- (3.6)}$$

$$m_{osc} = M_{piston} + M_{conrod''} \text{ ----- (3.7)}$$

The determination of the balancers outer radius is calculated using the formula below;

$$\rho = m_{osc}/V \rightarrow V = m_{osc}/\rho$$

$$V = \pi (R_2 - R_1)^2 H = m_{osc}/\rho \text{ ----- (3.8)}$$

where R_2 = outer radius;

H = balancer thickness = crankpin length;

R_1 = inner radius;

ρ = density of material of build of balancer

e) Testing

Minor experimentations were carried out for validation purposes. The fuel consumption test and the engine vibration test were both carried out and the results gathered were tabulated for comparison and analysis with the simulation results. Conclusions were made after the analysis.

3.3 Key Milestones

Table 3.1 outlines the key milestones of the entire project

TABLE 3.1: Key Milestones

Deliverable	Target Due Date	Description
Project proposal defence	14 July	Present the project proposal to supervisor and internal examiners.
Engine 3D model Generation	17 Aug	Complete the generation of 3D model of the engine in CATIA.
Interim Report Submission	22 Aug	Complete the documentation of the project as the interim report for FYP1
ADAMS, GT Power & Simulation	22 Sept	Execute the simulation and analysis for the balancers, the turbocharger and other engine parameters
Determination and Optimization of the Best Concept	18 Nov	Analysis the simulation results to determine the best concepts and optimize the results for better enhancement of engine
Project Finalization	8 Dec	Conduct experiments and validate the simulation results.

3.4 Gantt Chart

Task	Month	JUN				JUL					AUG				SEP				OCT					NOV				DEC	
	Week	1	2	3	4	1	2	3	4	5	1	2	3	4	1	2	3	4	1	2	3	4	5	1	2	3	4	1	2
	Duration	FYP I												Break				FYP II											
1	Project Title Confirmation	█																											
2	Problem Identification	█	█																										
3	Study & Research		█	█	█	█	█																						
4	Solution Generation & Finalization					█	█																						
5	Software & Equipment Handling Tutorial							█	█	█																			
6	Engine Dismantling & Dimensioning										█	█																	
7	CATIA 3D Modelling of Engine & Balancers											█	█																
8	GT Power Simulation of Cylinder Deactivation													█	█	█													
9	GT Power Simulation of Turbocharging														█	█	█												
10	ADAMS Simulation of Engine & Balancers															█	█												
11	Analysis of Simulation Results																		█	█	█								
12	Experimentation & Validation																			█	█	█							
13	Determination of Best Concepts																								█				
14	Optimization of Best Concepts																									█	█		
15	Project Finalization																										█	█	

CHAPTER 4

RESULTS AND DISCUSSION

4.1 Concept Generation

Several concepts of cylinder deactivation and forced induction system are proposed but they have to undergo GT Power simulation to determine their efficiency in terms of fuel consumption and engine performance to come out with the best combination.

The cylinder deactivation technology is made up of two main concepts; one with complete piston assemblies removal from the deactivated cylinders and the other has the piston remained inside. Complete removal of piston assemblies is a concept whereby the whole piston assemblies are removed, leaving an empty cylinder. The cam lobe of the targeted cylinders is grinded to roundness to keep the intake and exhaust valves closed at all time. The fuel injector of the targeted cylinders will be ceased from functioning by plugging off the wire socket to the injector, hence cutting off the input from the ECU. As for the proposal to keep the piston inside the targeted cylinder, the deactivation method only ceases the injection of fuel and sparks from the spark plugs.

For feasibility of the engine performance, only 1-cylinder and 2-cylinder deactivation are considered as 3-cylinder deactivation cannot generate enough power and torque for the car to run. It has been proven when 3-cylinder deactivation (piston remained) was tried on a PERODUA Myvi. The car engine could not be started or died seconds after ignition. Thus, this makes four cylinder deactivation concepts, which are 1- and 2-cylinder deactivation with complete piston assemblies removal as well as 1- and 2-cylinder deactivation with piston remained.

Concepts of forced induction systems are electric supercharging and turbocharging. Turbocharging however, has two different utilizations for the two different cylinder deactivation technology. For deactivation with piston removal, the exhaust from the two normal cylinders is used to turbocharge while for deactivation without piston removal, the exhaust from the deactivated cylinders are used for forced induction through a separated exhaust manifold.

4.2 Data Gathering

Standard engine parameters of K3-VE are acquired from the manufacturing sector through online information as well as manual measuring process. The data is required to model an engine map for the GT Power simulation to acquire results as close as possible to the actual K3-VE engine. Other common working parameters such as those factoring the combustion for SI engine are taken from the GT power examples, some through assumptions and engineering idealization. Data collected is summarized as below;

4.2.1 Online Information

Table 4.1 below summarizes all the important engine parameter values of K3-VE engine acquired online from car manufacturers.

TABLE 4.1: Engine Parameter Values Acquired Online

Compression Ratio	10:1	[23]
Bore X Stroke	72mm X 79.7mm	[23]
Con-rod Length	129.5mm	[7]
WristPin to Crank Offset	8mm	[7]
Valve Timing Intake Opening	30° to -12° BTDC	[7]
Valve Timing Intake Closing	10° to 52° ABDC	[7]
Valve Timing Exhaust Opening	30° BBDC	[7]
Valve Timing Exhaust Closing	2° ATDC	[7]
Intake Valve Lash	0.145 to 0.235mm (take 0.2mm)	[24]
Exhaust Valve Lash	0.275 to 0.365mm (take 0.3mm)	[24]

As for forced induction, compressor maps of turbocharger & electric supercharger is plotted into arrays to allow simulation in GT Power. The selected electric supercharger is the Phantom FTS VW 2.0 TQ-18024V which has been dyno tested according to the website, with the specifications and compressor maps in Appendix A. The turbocharger is selected from common models in the GT Power tutorials.

4.2.2 Manual Measurement and Computation

Based on the information on cylinder, TDC Clearance Height is calculated to be 2.2mm with calculation show in Appendix B. The cam profile on the camshafts of K3-VE engine is measured using the dial gauge for both the intake valves and exhaust valves to generate the approximate arrays of valve lifts v.s. degrees. Other piston assembly measurements are taken using vernier caliper for CATIA 3D modeling purposes.

4.3 GT Power Simulation and Analysis

4.3.1 GT Power K3-VE Engine Map Simulation

The engine map of the 4-cylinder gasoline engine is constructed in GT Power with all necessary engine parameters as shown in Figure 4.1 below.

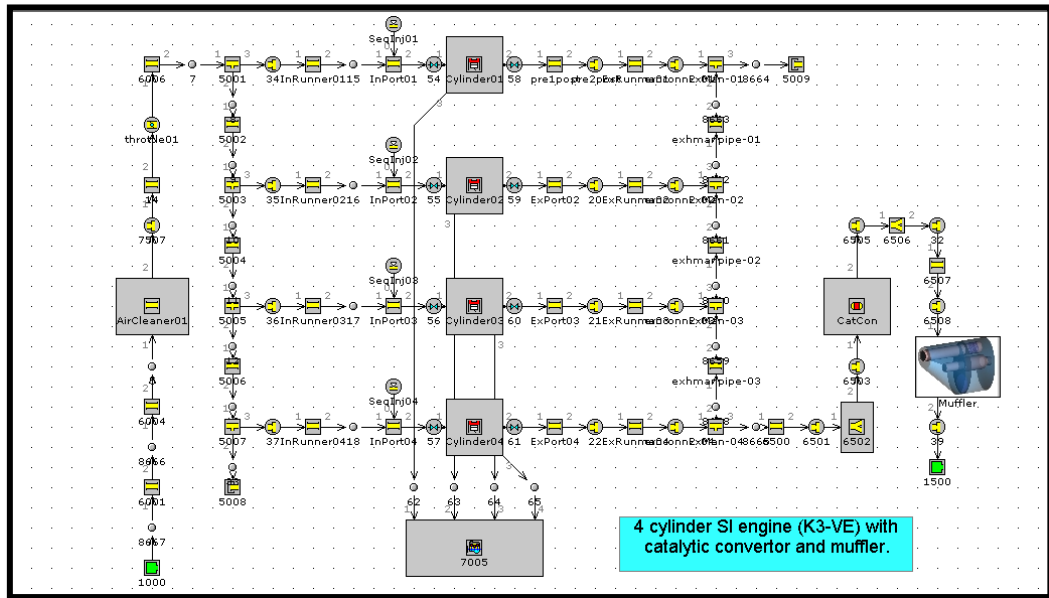


FIGURE 4.1: GT Power Engine Map of the K3-VE 4-Cylinder Gasoline Engine

The simulation is run to generate five graphs for analysis of the engine fuel consumption and performance. It is important to validate the simulation results by comparing the simulated engine brake power and torque curve to the actual manufacturing data acquired from the Figure 1.1. The comparison can be seen in both the figures below.

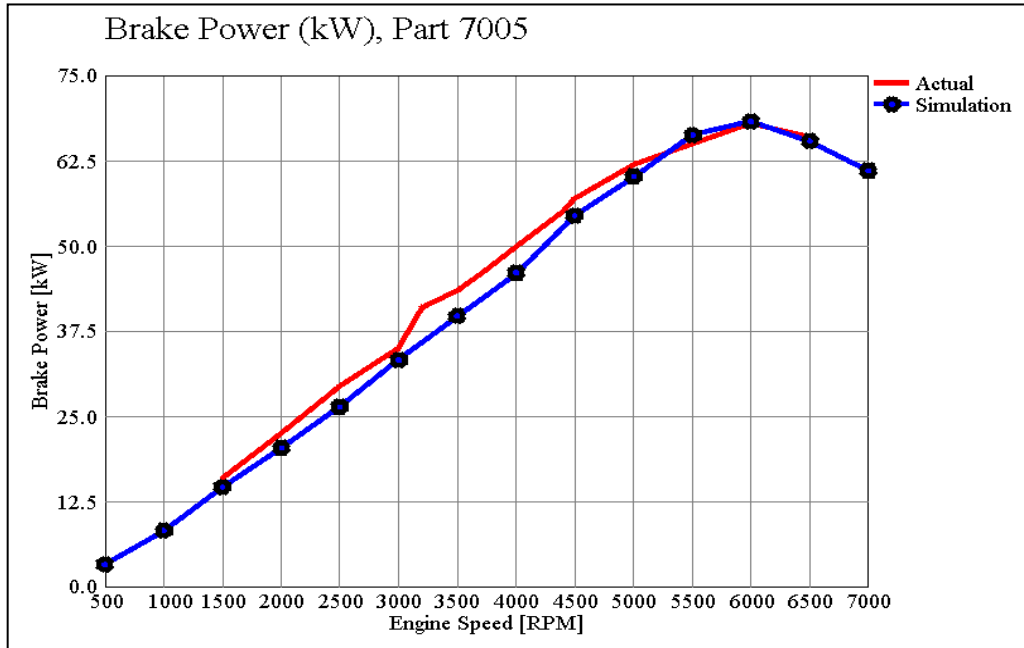


FIGURE 4.2: Brake Power Curve of the Actual and Simulated Engine

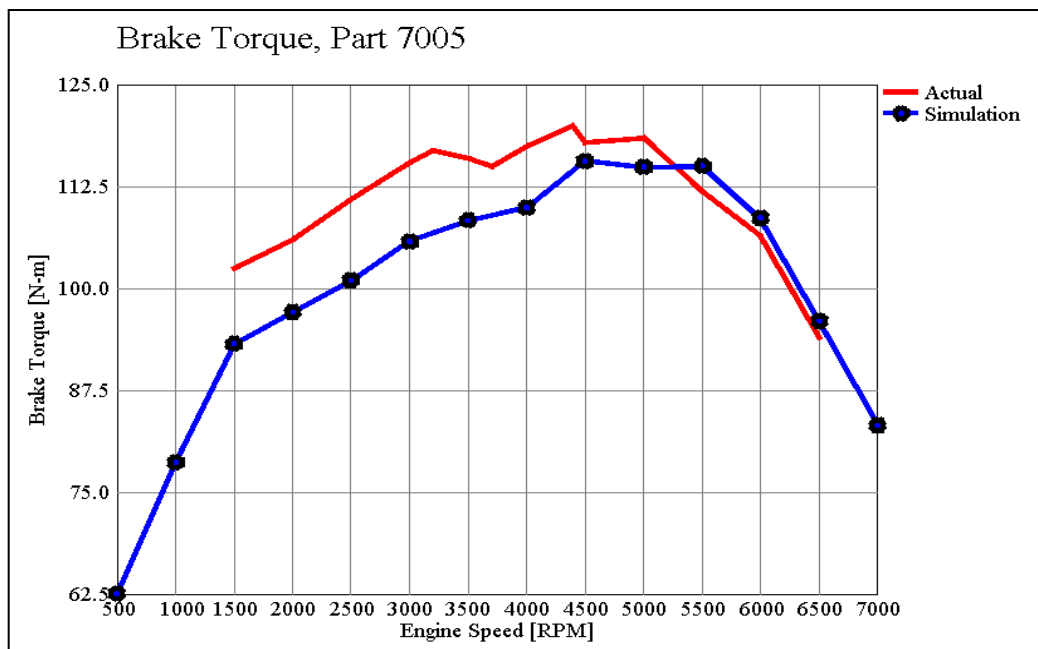


FIGURE 4.3: Brake Torque Curve of the Actual and Simulated Engine

The two figures above compare the actual brake power and torque curve of the 1.3L K3-VE engine with the simulated projection of brake power and torque of the GT Power Mapped Engine, with red line being the data obtained from manufacturer’s documents online. It is important to compare the two curves to validate the accuracy of the GT Power-mapped engine model. The smaller the percentage of errors, the higher the reliability of the simulation data for the subsequent modifications made. The difference of the values is computed in terms of percentage of errors in Table 4.2.

TABLE 4.2: Percentage of Error of Simulated Data

Engine Speed [RPM]	Brake Torque[N-m]		% of Error	Brake Power [kW]		% of Error
	Actual	Simulation		Actual	Simulation	
6500	94	96.0306	2.1%	66	65.366	1.0%
6000	106.5	108.64	2.0%	68	68.2605	0.4%
5500	112	115.045	2.6%	65	66.2614	1.9%
5000	118.5	114.931	3.1%	62	60.178	2.9%
4500	118	115.674	2.0%	57	54.5101	4.4%
4000	117.5	109.962	6.9%	50	46.0606	7.9%
3500	116	108.32	7.1%	43.5	39.7012	8.7%
3000	115.5	105.807	9.2%	35	33.2403	5.0%
2500	111	101.022	9.9%	29.5	26.4474	10.3%
2000	106	97.1142	9.1%	22.5	20.3396	9.6%
1500	102.5	93.2403	9.9%	16	14.6461	8.5%

It can be seen that the highest percentage of error is only about 10% which deems the GT Power engine model reasonably reliable to be used as reference of the actual outcome data.

Since the current 4-cylinder model’s reliability has been validated, every modification made to the model with the correct modification in engine mapping in GT Power will approximate the actual results as well.

4.3.2 GT Power Cylinder Deactivation Simulation

There are four different cylinder deactivation modules suggested which are 1 deactivated cylinder with complete piston assemblies removal, 1 deactivated cylinder with piston remained, 2 deactivated cylinders with complete piston assemblies removal as well as 2 deactivated cylinders with pistons remained. All the engine maps of the cylinder deactivation modules are inserted in Appendix C. The results of the simulation are portrayed in the following few figures.

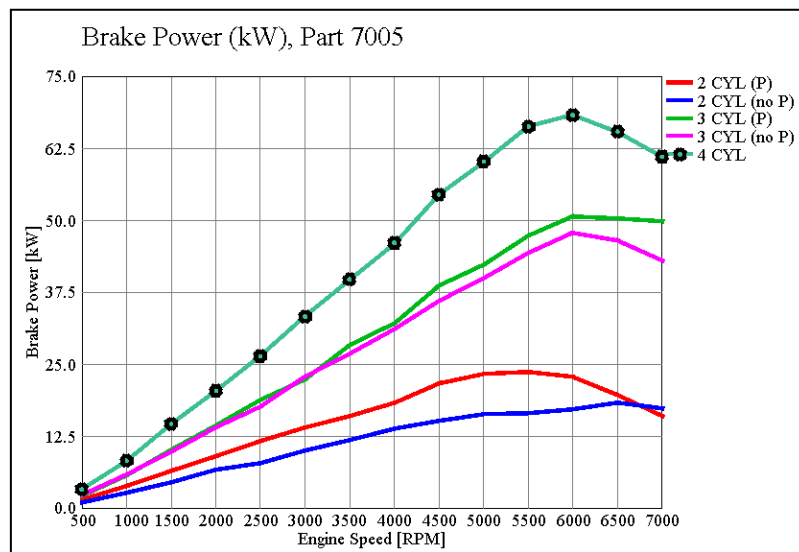


FIGURE 4.4: Brake Power Curve of Different Cylinder Deactivation Methods

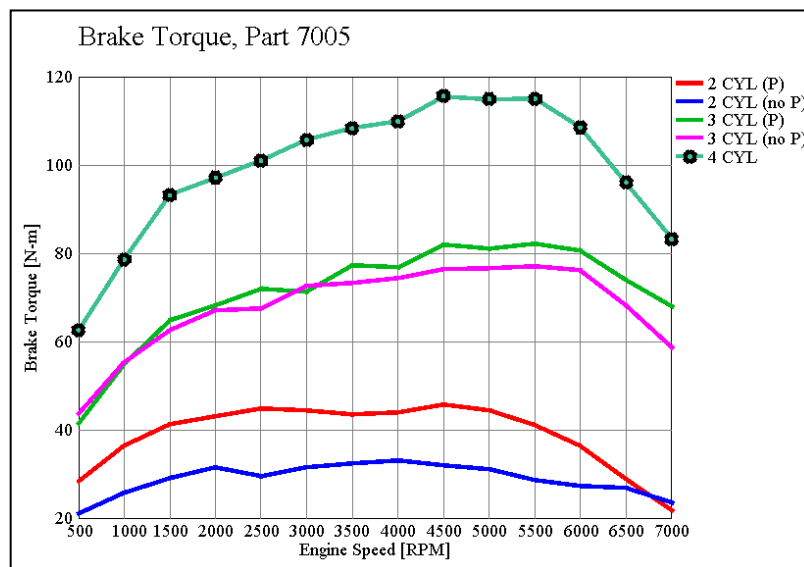


FIGURE 4.5: Brake Torque Curve of Different Cylinder Deactivation Methods

Figure 4.4 and 4.5 show that overall brake power and torque of the engine drops with the increasing number of deactivated cylinders. Between the two cylinder deactivation methods, those with piston removal have a relatively lower power and torque as well.

As for fuel consumptions, Figure 4.6 shows that the total fuel consumption decreases with increasing number of cylinder deactivation. Between the two methods, cylinder deactivation with piston removal consumes much less fuel. The total fuel consumption of cylinder deactivation method with the piston remained is almost equal to those of a four cylinder engine because a lot of fuel is consumed to compensate for the pumping loss of the engine as power is wasted on drawing air in from the intake manifold.

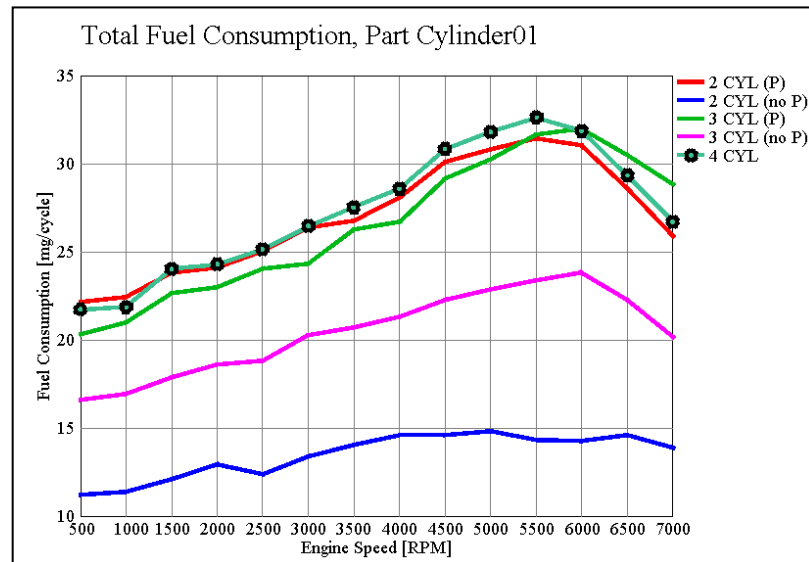


FIGURE 4.6: Total Fuel Consumption Per Cylinder of Different Deactivation Methods

The total fuel consumption patterns of cylinder deactivation are validated through the fuel consumption test on a PERODUA Myvi. The test was run through two engine conditions, (1) normal engine (2) 1-cylinder deactivation. The cylinder deactivation was done on the 3rd cylinder in order to synchronize with the model in GT Power. The piston remained inside the cylinder. The wire socket connecting the fuel injector for the targeted cylinder is plugged off.

The car was pumped full tank and driven over a designated course as shown in Appendix F. At the end of the course, the car was pumped full tank again to determine the amount of the fuel used up. The results are tabulated in Table 4.3 and illustrated in graph in Figure 4.7. Although Figure 4.6 shows fuel consumption by engine while 4.7 indicates fuel consumption by car which takes into account the driving style of drivers, the drive cycles, drivetrain efficiency, etc, the patterns should remain the same as the factors are all made to be as constant as possible by setting the same engine rpm over the same route.

It can be seen that the patterns are similar to those in Figure 4.6 where there is a slight decrease in fuel consumption for the engine with 1-cylinder deactivation, justifying that fuel consumption decreases with number of cylinder. Moreover, the fuel consumption increases relatively steeper at 3500 rpm.

TABLE 4.3: Fuel Consumption of Car over Driving Course of 27.7km

	RPM	RM for full tank	RM/liter	fuel used (liter)	Average (liter)	Mileage (km/litre)	Average (km/litre)
4 CYL	2000	4.25	2.10	2.024	2.090	13.69	13.26
	2000	4.53	2.10	2.157		12.84	
	2500	4.56	2.10	2.171	2.198	12.76	12.61
	2500	4.67	2.10	2.224		12.46	
	3000	4.88	2.10	2.324	2.329	11.92	11.90
	3000	4.90	2.10	2.333		11.87	
	3500	5.20	2.10	2.476	2.440	11.19	11.35
	3500	5.05	2.10	2.405		11.52	
3 CYL	2000	4.20	2.10	2.000	1.983	13.85	13.97
	2000	4.13	2.10	1.967		14.08	
	2500	4.20	2.10	2.000	2.090	13.85	13.28
	2500	4.58	2.10	2.181		12.70	
	3000	4.80	2.10	2.286	2.231	12.12	12.42
	3000	4.57	2.10	2.176		12.73	
	3500	4.90	2.10	2.333	2.405	11.87	11.53
	3500	5.20	2.10	2.476		11.19	

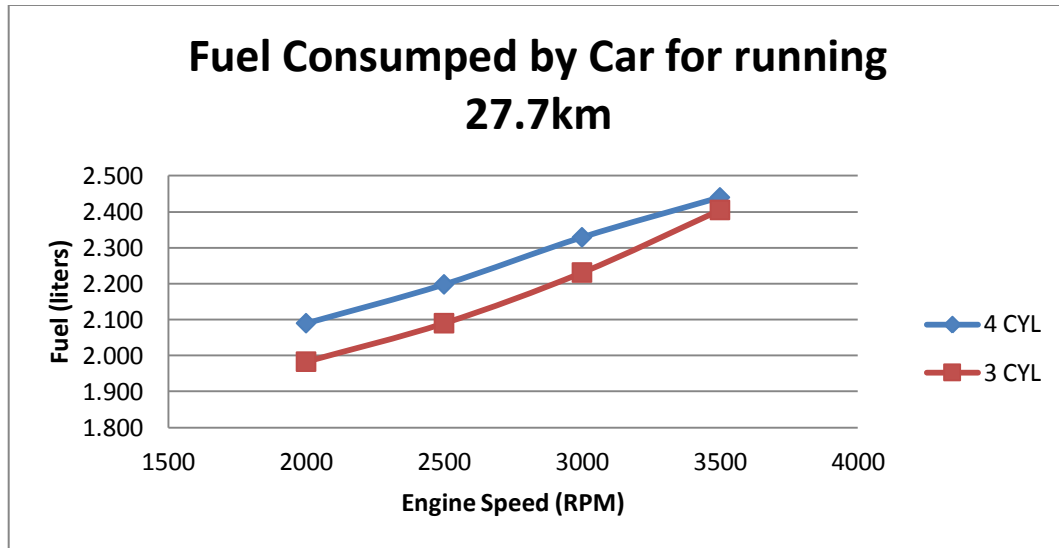


FIGURE 4.7: Total Fuel Consumed by 1.3L Myvi under Different Engine Condition

The BSFC and Brake Efficiency graphs in Figure 4.8 and 4.9 clearly shows that cylinder deactivation with piston removal has better efficiency. Again, it is due to the pumping loss theory. On the other hand, they even have better efficiency than the normal 4-cylinder engine. It is mainly because each cylinder causes a drop in efficiency as energy is transferred from one form to the other and a lot of energy is wasted through the process. As the number of cylinder decreases, so does the waste in energy, hence resulting in an overall higher efficiency.

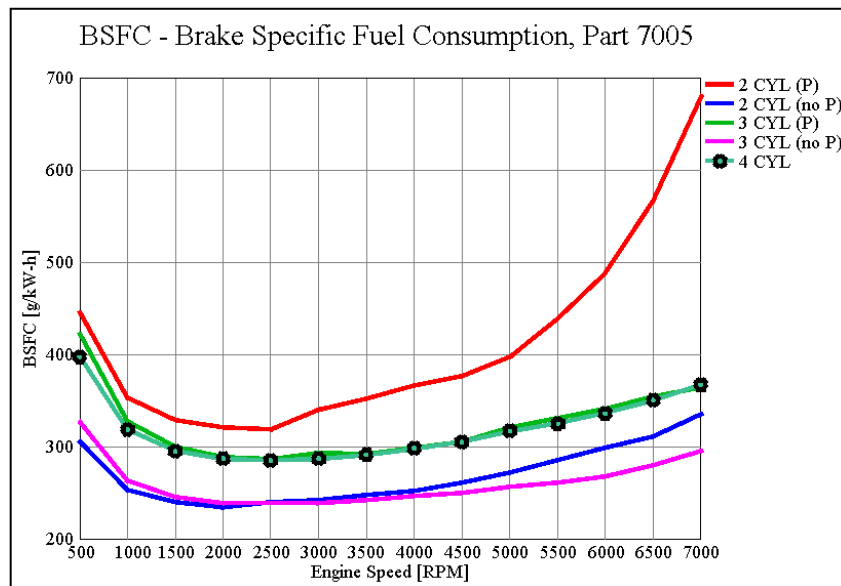


FIGURE 4.8: BSFC Graph of Different Cylinder Deactivation Methods

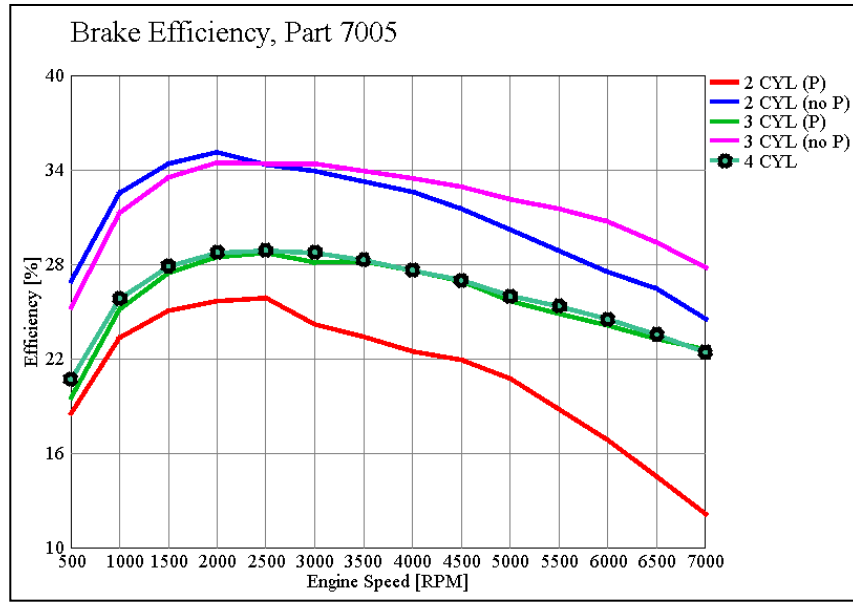


FIGURE 4.9: Brake Efficiency of Different Cylinder Deactivation Methods

The optimum power and torque requirement of the engine for this project is focused on the requirement of a city car. It is computed to require engine power of 18.2 kW and engine torque output of 89.6 Nm in Appendix D with the requirement considering the car being able to be driven by a driver with four other passengers on flat normal asphalt road surfaces at constant speed of 110km/h (requiring power of 18.2kW and torque of 89.6Nm) and up a slope of 5.7° at a constant speed at 30km/h (requiring power of 12.3kW and torque of 63.3Nm). Since the power and torque can be enhanced through the employment of supercharger or turbocharger later on, not all cylinder deactivation methods that do not meet the requirements are cancelled out immediately. Instead, decision is made with consideration for the forced induction system.

The initial feasibility evaluation of engine deems 2-cylinder deactivation incapable of delivering the required performance as they only have a maximum torque of about 45Nm which is only 50% of the required torque. Even with turbocharging or supercharging, the required torque will not be achieved. Hence only both 1-cylinder deactivation methods are adopted to be combined with forced induction systems.

4.3.3 GT Power Cylinder Deactivation with Forced induction Simulation

As mentioned in section 4.1, there are three types of forced induction systems in combination with the 1-cylinder deactivation methods which are (1) 1-cylinder deactivation (piston removal) employed with electric supercharger (2) 1-cylinder deactivation (piston removal) employed with turbocharger and (3) 1-cylinder deactivation (piston remained) employed with turbocharger. All their GT Power engine maps are in Appendix E. The simulation results are as follow;

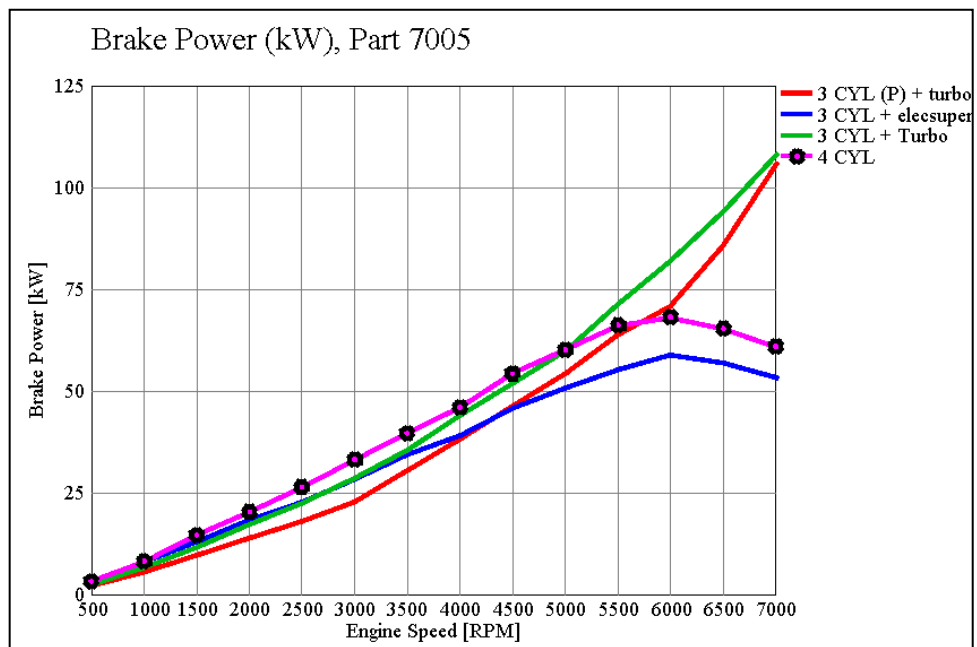


FIGURE 4.10: Brake Power Curve of Different Combinations

In terms of engine performance, from Figure 4.10 and 4.11, it is seen that method (1) has a relatively lower but steady power and torque curve. Its curve pattern is almost similar to that of the normal engine, mainly because an electric supercharger provides a constant boost in air pressure. It is powered by an external power source, like a battery so it does not drive power off the engine which results in higher fuel consumption and engine wear.

As a whole, method (2) has the best power and torque performance out of the three but it only exceeds the normal engine at high engine speed. It can be seen that initially at lower engine rpm, the power and torque increases slowly mainly because of at lower

engine rpm, the exhaust gases are in little amount and hence the effect of turbo charging is low as well. The effect increases in higher rate with increasing engine speed gradually.

Method 3 proves to be the least effective at lower rpm but its performance enhances at higher engine speed. It is because the turbo charging mechanism is only powered by the exhaust gases of one single cylinder. Moreover, the pumping loss contributes to a lower power and torque. Hence it has the same curves as the conventional turbocharging mechanism but of a lower value. And at engine speed of 6000rpm and onwards, method (3) continues to increase as it is not affected by the backpressure due to the flow restriction because only exhaust pressure from one cylinder is used to power the turbocharger of the same capacity.

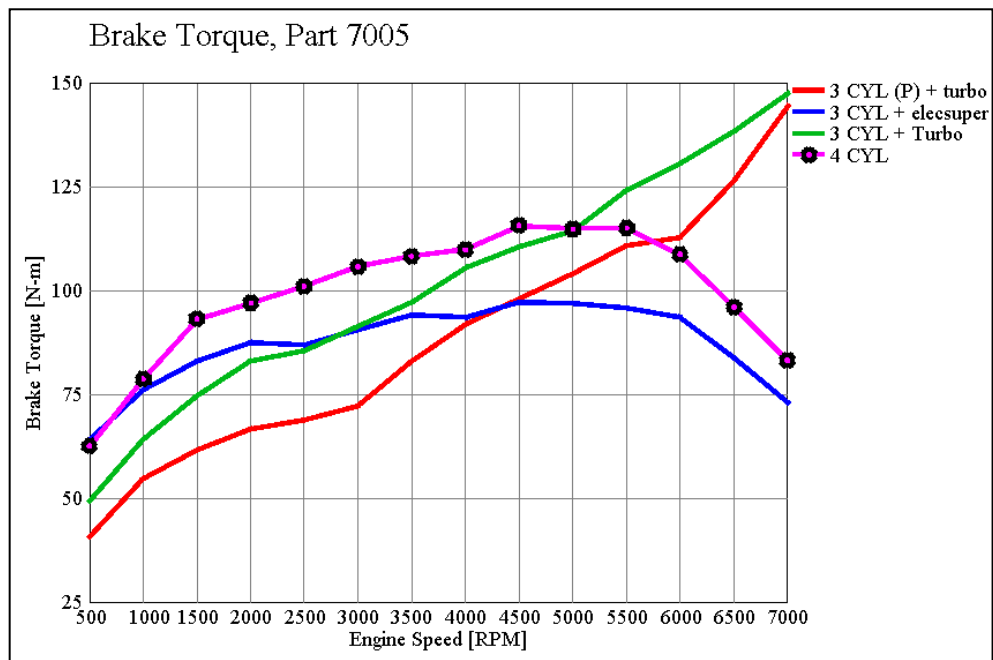


FIGURE 4.11: Brake Torque Curve of Different Combinations

For fuel consumption evaluation, it is deduced from Figure 4.12 that fuel consumption rate is almost proportional to the engine power and torque. The higher the power produced, the more the fuel consumed. For a better evaluation of the data, BSFC and brake efficiency graph are more helpful as the electric supercharger and turbocharger are of different specifications and hence it will be fair to evaluate based on their efficiency.

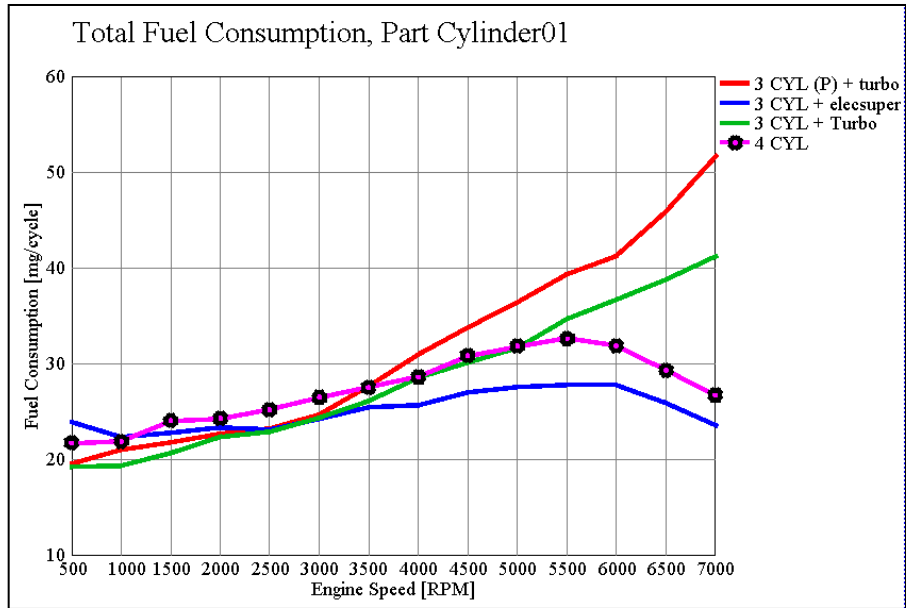


FIGURE 4.12: Total Fuel Consumption of Different Combinations

Different from the results shown from the previous graph, the normal engine has the highest BSFC value and the lowest efficiency after the engine hits speed of 3500rpm. Method (3) performs with lowest efficiency and has highest BSFC at lower engine speed.

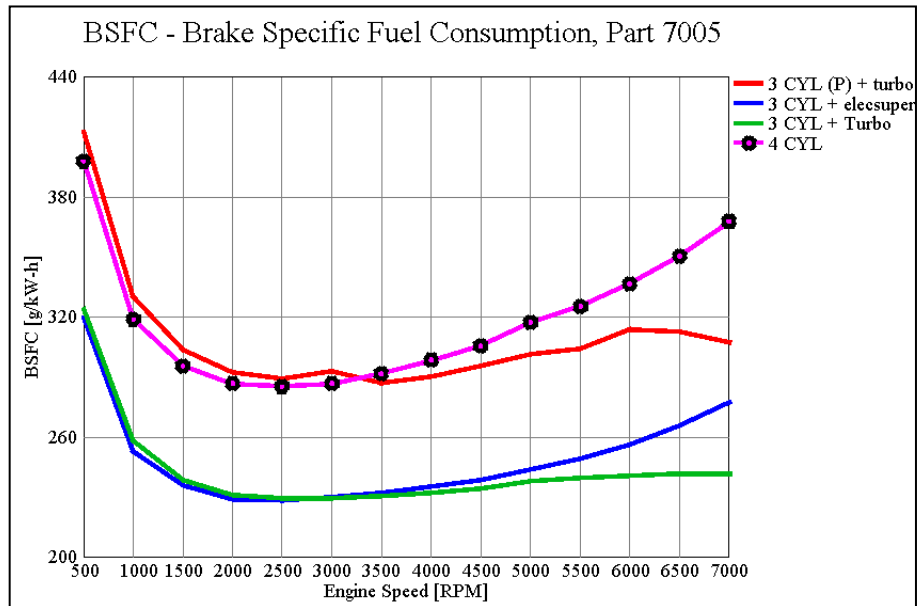


FIGURE 4.13: BSFC of Different Combinations

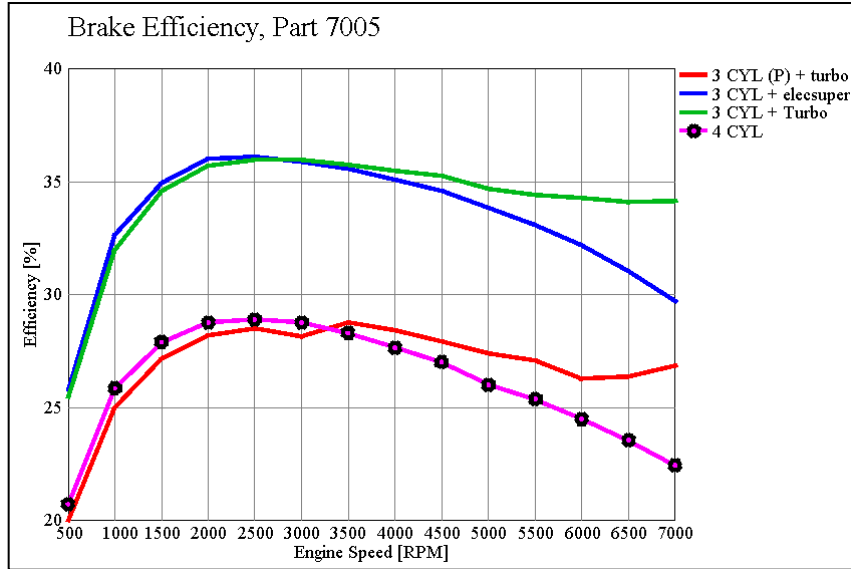


FIGURE 4.14: Brake Efficiency of Different Combinations

Method (1) and (2) have the higher efficiencies and hence lower BSFC. At lower rpm, Method (1) outweighs method (2) but method (2) has a relatively better performance at higher rpm. It is mainly because method (2) uses a turbocharger has turbo lag where the effects are only visible after the breaking point where sufficient exhaust pressure is built to run the turbine efficiently. As for method (1), the efficiency drops at higher rpm because its compressor is running at a constant speed while the compressor in method (2) runs at speed proportional to exhaust pressure, which increases with engine speed.

Before concluding on the best concepts, it is important to double check the power and torque requirement set early on as in Appendix D showing an engine power requirement of 18.2kW and an engine torque output of 89.6Nm. All the three methods fulfill the requirements and are all eligible to be selected as the best concepts.

Moreover, it is also necessary for the identification of the average engine speed range or the speed range in which the engine will be running in most occasions or frequency. The reason is to allow the comparison of different concepts pinpointed in a focused area in a more realistic and analytical manner. Under EPA standards, the average speed of a car is approximately 30.4km/h for UDDS [25] while the HWFET records an average speed of 77.7km/h [26]. Using formula 3.1, the average engine speed is computed based on average vehicle speed and tabulated in Table 4.4.

TABLE 4.4: Average Engine Speed for UDDS and HWFET using Different Gears

Driving Cycle		UDDS	HWFET
CAR SPEED	km/h	30.40	77.70
	m/s	8.44	21.58
Gear	Gear Ratio	Engine Speed (RPM)	
1	3.182	1878	4800
2	1.842	1087	2779
3	1.250	738	1886
4	0.865	511	1305
5	0.750	443	1131

As table 4.4 indicates, the range of engine speed is approximately between 443rpm to 4800rpm. However, it is not efficient for the car to be running 30.4km/h using gear higher than 3rd gear while a speed of 77km/h should be driven with the 3rd, 4th or 5th gear. Hence, considering both UDDS and HWFET driving cycles, the average engine speed falls in the range of 700rpm to 2000rpm, which is made as the focus of study.

By focusing on engine speed range of 700rpm to 2000rpm which are low speed range, it is seen that method (1) has slightly higher brake efficiency and a lower BSFC. Given an electric supercharger with the same specifications of the turbocharger, the total fuel consumption should be lower, producing a slightly higher power and torque within the lower engine speed range.

Hence, the best concept should be method (1) for a city car. If the project is opted for a sports car which have engine frequently running at higher rpm, method (2) will be the best fit.

4.4 ADAMS Simulation and Analysis

As Method (1) has been selected for this project, it is important to look into the vibration levels of the engine to ensure customers comfort. Method (1) adopts cylinder deactivation method with complete removal of the piston assembly from the targeted cylinders. Balancing will be carried out in terms of single cylinder mass balancing as well as multi-cylinder cranktrain balancing. Consider adopting a 2-cylinder deactivation, the first step will be to balance the multi-cylinder cranktrain as much as possible. Then single cylinder mass balancing process is required.

An alternative engine has been disassembled in a workshop and the engine parameters of that particular engine in the lab has been recorded and utilized for the simulation of the cylinder deactivation methods. The results of the simulation are elaborated in the upcoming subsection. Formulas are utilized for computation of the required mass of the balancers as well in order to determine the dimensions and material of the balancers.

A vibration test was conducted to validate the effect of cylinder deactivation on engine vibration level as specified in Appendix G. The test however did not get results of the vibration of the crankshaft but the vibration of the surface of the engine which theoretically is proportional to each other. The vibration level is shown in Table 4.5.

TABLE 4.5: Tabulated Results of Vibration Test

Engine Condition	y			x			z		
	Up	Low	Amp.	Up	Low	Amp.	Up	Low	Amp.
Normal	90	-170	260	55	-40	95	55	-80	135
Deactivation	600	-220	820	130	-100	230	115	-125	240
Difference			560			135			105

It is seen that the vibration level increases for every axes by quite a big margin with two cylinder deactivation, especially in the y-axis (refer to Appendix G for illustration of axes), justifying that cylinder deactivation increases the vibration level of the engine and hence balancing has to be carried out to counter the rise in vibration amplitude to ensure comfort of the driver and passengers.

4.4.1 Balancers

It is necessary to balance the four cylinder inline engine after two pistons are removed from the cranktrain. Balancers of design weight and dimension can be mounted on the crankpin of the deactivated cylinders to balance off the uneven forces and moments. Using both Multi-Cylinder CrankTrain Balancing and Single Cylinder Mass Balancing, the desired balancers dimensions can be determined.

From formula (3.6),

$$M_{\text{conrod}} = 0.755\text{kg} (58.392\text{mm}/145.88\text{mm}) = 0.3022\text{kg}$$

From formula (3.7),

$$m_{\text{osc}} = 1.217\text{kg} + 0.3022\text{kg} = 1.5192\text{kg}$$

The desired material is stainless steel which is strong, durable and will not rust, which is suitable for a balancer inside the engine because it is really hard to overhaul the engine for parts replacement. Density of stainless steel is provided in CATIA as 8.031×10^{-6} kg/mm³. Assuming the balancers are made into a cylinder with a hole that fits onto the crankpins with a thickness of 22mm, the outer diameter required is;

From formula (3.8),

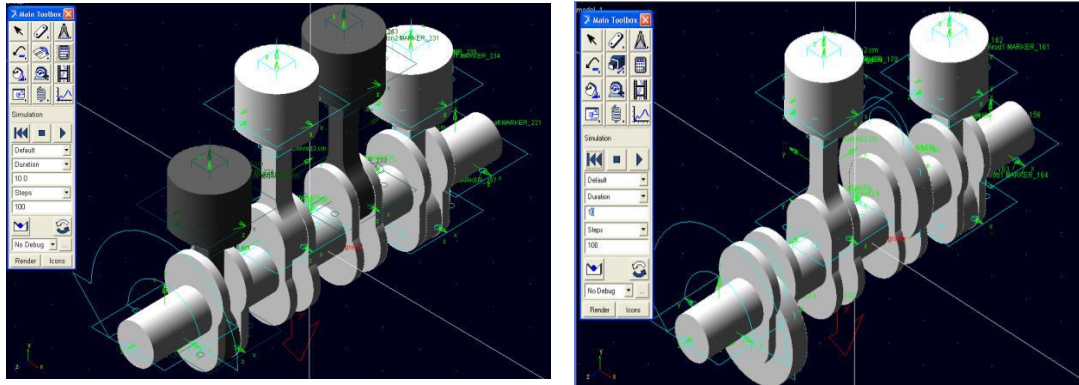
$$\pi (R_2 - 22.5\text{mm})^2 (22\text{mm}) = 1.5192\text{kg} / (8.031 \times 10^{-6} \text{ kg/mm}^3)$$

$$R_2 = 78.154\text{mm}$$

Hence the balancers should be made of stainless steel with a cylindrical shape with outer diameter of 78.154mm, drilled with a central hole of the crankpin diameter. They should have a thickness of 22mm and be split in halves to enable mounting. Nut and bolts mechanism can be made the fastening mechanism of the halves of balancers.

4.4.2 CATIA and ADAMS Simulation

Based on the dimension selected for the balancer as well as all the engine parts dimension measured in the workshop, CATIA is used for modeling of the engine components. The models are inserted into ADAMS with specified constraints for simulation of the vibration forces and moments of the crankshaft.

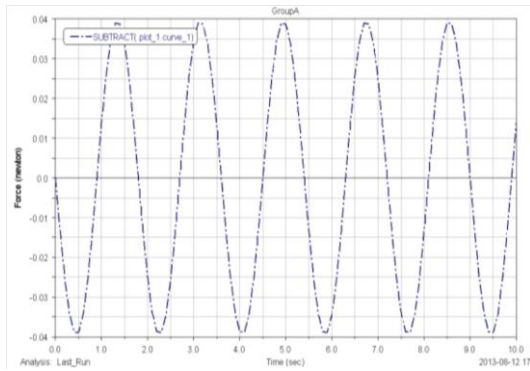


(a) Piston 1 & 3 Deactivated

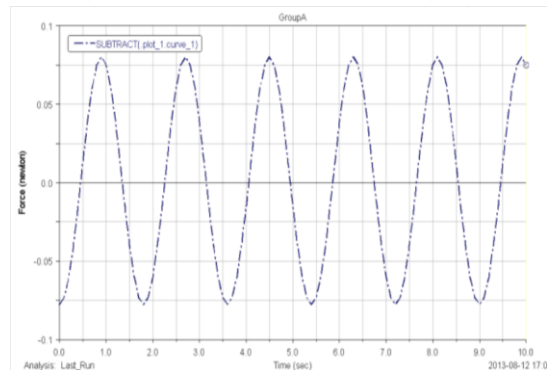
(b) Cylinder Deactivation with Balancers

FIGURE 4.15: ADAMS View of Cylinder Deactivation and Balancing

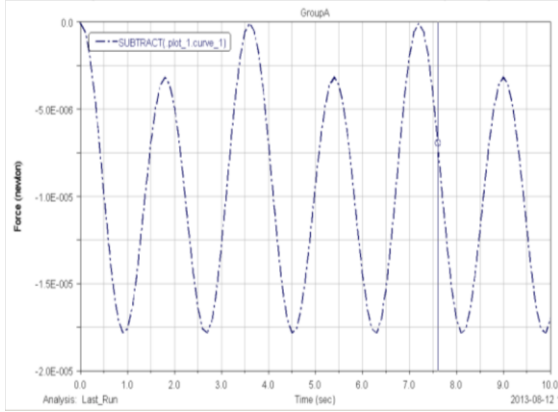
The results are represented by the graphs below which is summarized in Table 4.6, allowing comparison and analysis of the results for normal crankshaft, crankshaft with cylinder deactivation as well as crankshaft with cylinder deactivation and balancers. Figure 4.16 shows that only the magnitude of vibration in the y-direction is significant for the analysis, as y-direction is the direction of crank throws. Vibration in z-direction is almost zero while vibration forces in x-direction are small and hence negligible.



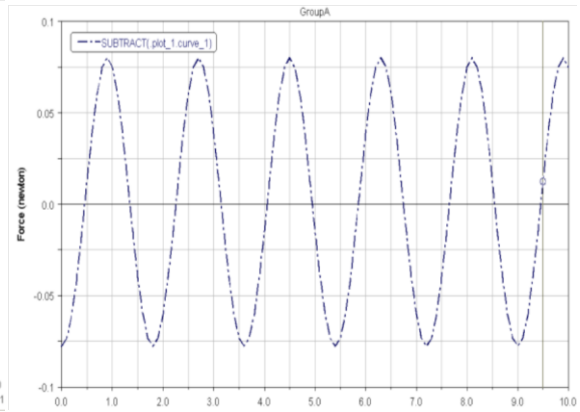
(a) Magnitude of Vibration (x-direction)



(b) Magnitude of Vibration (y-direction)



(c) Magnitude of Vibration (z-direction)



(d) Magnitude of Vibration (Total)

FIGURE 4.16: Resultant Magnitude of Vibration of Crankshaft of the Normal Engine

Figures 4.17 and 4.18 show the magnitude of vibration in the y-direction for the engine with 2-deactivated cylinders and the engine with 2-deactivated cylinders but mounted with balancers.

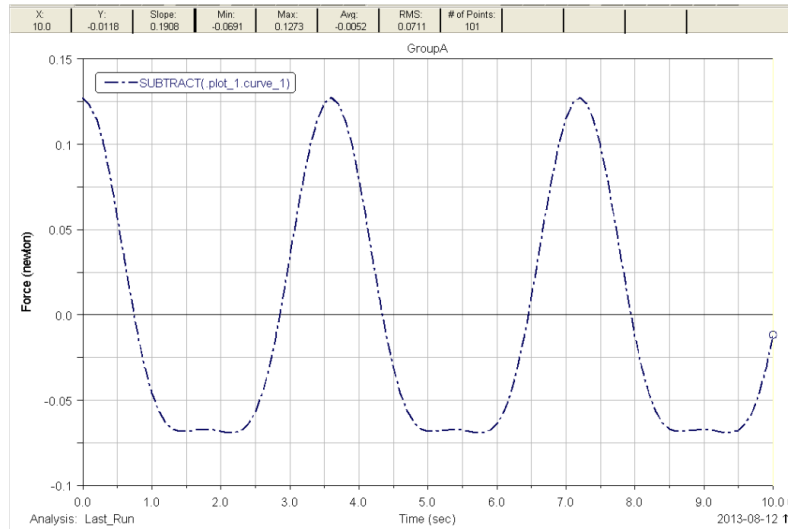


FIGURE 4.17: Magnitude of Vibration of Crankshaft with 2 Deactivated Cylinders

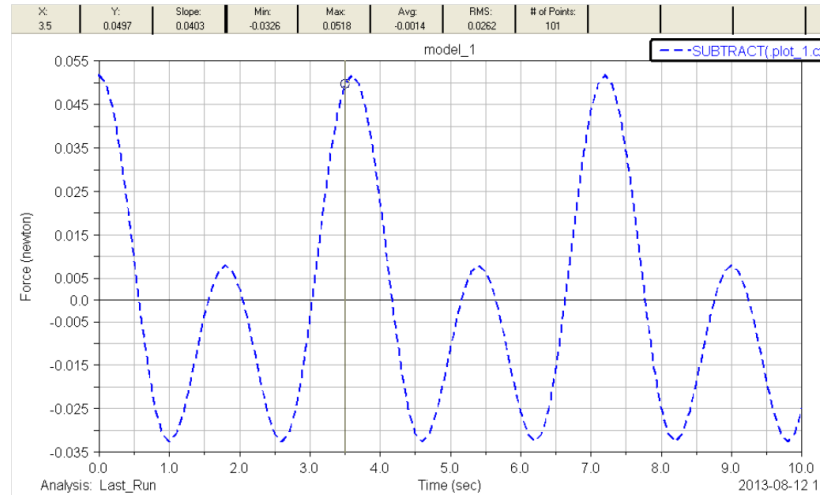


FIGURE 4.18: Vibration of Crankshaft with Balancers for Cylinder Deactivation

The vibration amplitude is the difference between the maximum and minimum value of force. In the y-axis, the vibration amplitude for each case is tabulated below. As shown in table 4.6, the balancers decrease the vibration amplitude from 0.1964N to only 0.0444N.

TABLE 4.6: Tabulated Results of Vibration Amplitude in ADAMS Simulation

Condition	Vibration Amplitude
• Crankshaft of a Normal 4-Cylinder Engine	0.1584N
• Crankshaft with 2 Deactivated Cylinders	0.1964N
• Crankshaft with Balancers for Cylinder Deactivation	0.0444N

As to calculate the resultant moment along the crankshaft, the results are simulated through a series of steps as specified in Appendix H. The resultant moment of crankshaft of the deactivated engine without balancing effort is plotted into graph by ADAMS in Figure 4.19 while Figure 4.20 shows the resultant moment of the crankshaft for the cylinder deactivated engine with balancing initiative.

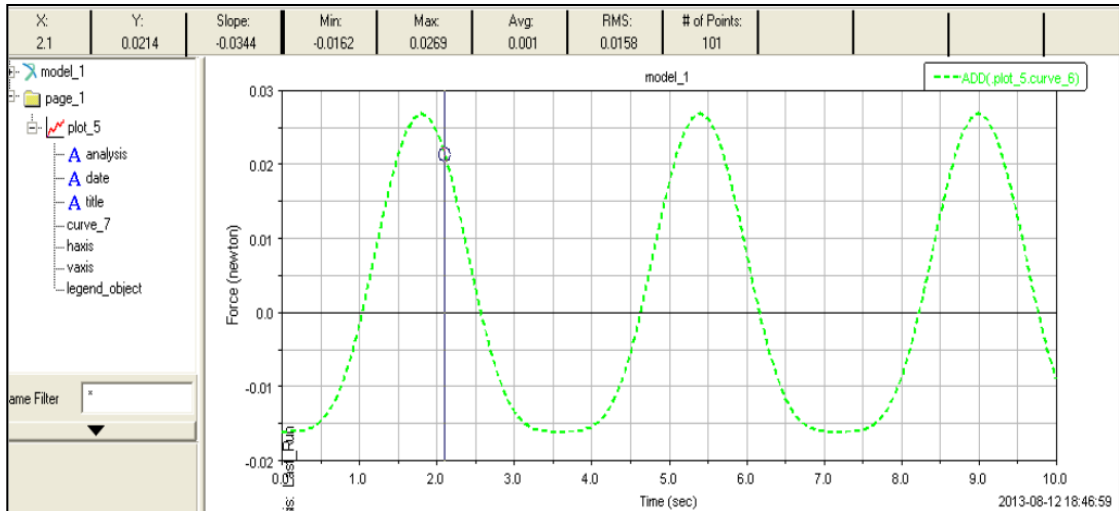


FIGURE 4.19: Resultant Moment of Crankshaft (Without Steel Balancer)

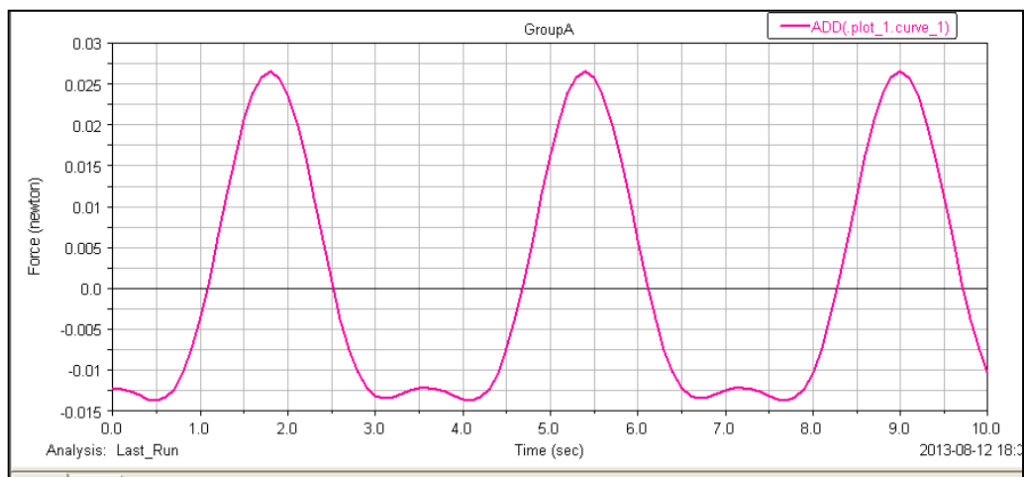


FIGURE 4.20: Resultant Moment of Crankshaft (With Steel Balancer)

Figure 4.19 shows a resultant moment of amplitude 0.0431N.m while Figure 4.20 shows a resultant moment of amplitude 0.0415N.m. As compared, the balancer only decreases the resultant moment of the crankshaft by a small margin. As a conclusion, balancing effort decreases both vibration forces and moments along the crankshaft.

CHAPTER 5

CONCLUSION AND RECOMMENDATION

5.1 Conclusion

As a conclusion, both objectives of the projects have been achieved by the best concept selected which is to employ 1-cylinder deactivation with complete piston removal to reduce fuel consumption and increase the engine power and torque with an electric supercharger powered by an external battery. The combination of cylinder deactivation and forced induction system has managed to enhance the overall efficiency of the engine too. Balancers can be mounted onto the crank pins of the deactivated cylinder which proves to be effective in reducing the vibration level rise due to the cylinder deactivation initiative. The project has been completed according to schedule although there are some delays around the November period of the Gantt chart due to unforeseen circumstances. Some aspects of the projects have been compromised due to time and monetary concerns as well. All in all, the project has managed to produce a desirable outcome, probing for further experimentation works for engine enhancement.

5.2 Recommendation

As the project is ended up till simulation stages, the next step is to put the best concept into experimentation to determine the degree of reduction in fuel consumption as well as the degree of enhancement in engine performance. It is important to determine if the modification to the engine will be feasible in economic, social and environmental sense to achieve high sustainability.

As seen in the simulation results, the electric supercharger in its current technology only induces limited gain in power and torque although it proves to have a better efficiency. Even with the best efficiency, if it produces outcomes with an overall lower power and torque that cannot meet the people's demand, it will not be marketable as well. Hence, along with technological development, electric supercharger with economical prices that runs at higher rpm can be manufactured to provide a higher boost. The balancing efforts can be repeated with better consideration of other factors to achieve better results as well.

Actually, since electric supercharger is a unit on its own, we can have one electric supercharger for each cylinder by having a separated intake manifold so the engine can achieve higher power and torque. It also allows separate controls of the supercharger if necessary. However more units mean more batteries and surely consume more spaces required in the car's front compartment.

REFERENCE

- [1] Lim, A. (2013). *Perodua Eco Challenge 2013 launched – 10 teams to battle it out to see who can best redesign a Myvi*. Retrieved June 8, 2013 from <http://paultan.org/2013/05/31/perodua-eco-challenge-2013-redesigning-a-myvi/>
- [2] Hofmann, T. (2006). *Cylinder Deactivation: Another Technology for Reducing Fuel Consumption*. Retrieved June 11, 2013 from http://www.moto123.com/imprimer_article.spy?artid=60250
- [3] Peters, G. (2007). *Cylinder Deactivation on 4 Cylinder Engines: A Torsional Vibration Analysis*. Retrieved June 11, 2013 from <http://alexandria.tue.nl/repository/books/658524.pdf>
- [4] AviationPros. (2005). *Turbocharging 101: Some History and Basics of Turbocharging Systems*. Retrieved June 12, 2013 from <http://www.aviationpros.com/article/10385857/turbocharging-101-some-history-and-basics-of-turbocharging-systems>
- [5] Ferguson, C. R. & Kirkpatrick, A. T. (2001). *Internal Combustion Engines (2nd ed.)*. New York, NY: John Wiley & Sons, Inc.
- [6] PERODUA (2013). Myvi Specifications. Retrieved June 12, 2013 from <http://www.perodua.com.my/ourcars/myvi/specifications>
- [7] Toyota Peru Intranet (n.d.). *Daihatsu Data: 3SZ-VE/K3-VE – Toyota*. Retrieved June 13, 2013 from http://intranet.toyotaperu.com.pe/tdp_sit/data/DAIHATSU/TERIOS/TERIOS_SHORT/pdf/manual/9514/D55B-2-E.pdf
- [8] Berndt, R. (2010). *The Variables of Valve Timing*. Retrieved June 19, 2013 from http://www.underhoodservice.com/Article/74456/tech_feature_the_variables_of_valve_timing.aspx
- [9] Christine & Gable, S. (2013). *Cylinder Deactivation. The Magic of Variable Displacement Engines*. Retrieved June 19, 2013 from <http://alternativefuels.about.com/od/researchdevelopment/a/cylinderdeact.htm>
- [10] J. D. Power and Associates. (2012). *Engine-Cylinder Deactivation Saves Fuel*. Retrieved June 19, 2013 from <http://autos.jdpower.com/content/consumer-interest/gnHI9wQ/engine-cylinder-deactivation-saves-fuel.htm>

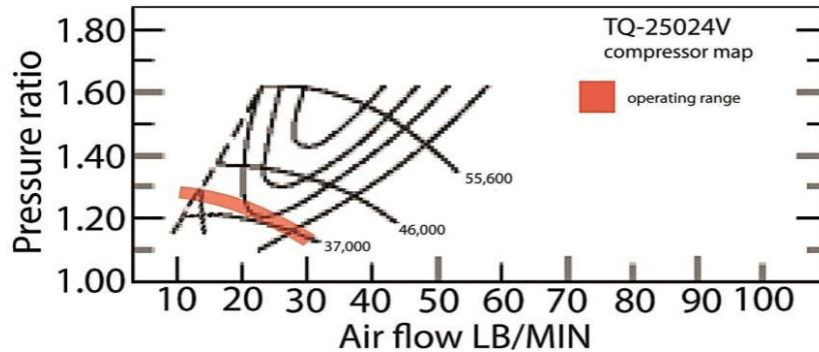
- [11] Bickerstaffe, S. (2011). *Automotive Engineer: Volkswagen cuts its four cylinder losses*. Retrieved June 20, 2013 from <http://ae-plus.com/news/volkswagen-cuts-its-four-cylinder-losses>
- [12] Niedermeyer, E. (2011). *The Truth About Cars: Are You Ready For A Mass-Market, Variable-Displacement Four-Cylinder?* Retrieved June 20, 2013 from <http://www.thetruthaboutcars.com/2011/09/are-you-ready-for-a-mass-market-variable-displacement-four-cylinder/>
- [13] Roth, D. (2006). *Auto News: Behold the cam-less future*. Retrieved June 23, 2013 from <http://www.autoblog.com/2006/12/22/behold-the-cam-less-future/>
- [14] Erb, J. (2012). *Lextreme: How Forced Induction Work*. Retrieved June 23, 2013 from <http://www.autoblog.com/2006/12/22/behold-the-cam-less-future/>
- [15] Ganesan, V. (2004). *Internal Combustion Engines (2nd ed.)*. Singapore, SG: Tata McGraw-Hill Publishing Company Limited.
- [16] Pulkrabek, W. W. (2004). *Engineering Fundamentals of the Internal Combustion Engine (2nd ed.)*. Upper Saddle River, NJ: Pearson Education, Inc.
- [17] Oagana, A. (2010). *How Anti-Lag Systems Work*. Retrieved July 8, 2013 from <http://www.autoevolution.com/news/how-anti-lag-systems-work-25222.html>
- [18] Wan, M. (2011). *Turbocharging : Twin-turbo*. Retrieved July 8, 2013 from http://www.autozine.org/technical_school/engine/Forced_Induction_3.html
- [19] Holloway, H. (2012). *Audi Reveals Electric Turbocharger Technology*. Retrieved July 8, 2013 from <http://www.autocar.co.uk/car-news/motoring/audi-reveals-electric-turbocharger-technology>
- [20] Richard, M. G. (2009). *Electric Supercharger Boosts Torque 50% and Reduces CO₂ by 20%*. Retrieved July 9, 2013 from <http://www.treehugger.com/cars/electric-supercharger-boosts-torque-50-and-reduces-co2-by-20.html>
- [21] Edgar, J. (2010). *Is This Your Electric Supercharger?* Retrieved July 9, 2013 from http://www.autospeed.com/cms/A_112129/article.html
- [22] Carspector (2013). *Perodua Myvi 1.3*. Retrieved July 26, 2013 from <http://carspector.com/car/perodua/000781/>
- [23] Automobile-Catalogue (2013). *2011 Perodua Myvi Specifications*. Retrieved July 26, 2013 from <http://www.automobile-catalog.com/make/perodua/myvi/myvi/2011.html>

- [24] Toyota Peru Intranet (n.d.). *Daihatsu Data: Valve Clearance (K3-VE)*. Retrieved July 31, 2013 from http://intranet.toyotaperu.com.pe/tdp_sit/data/DAIHATSU/TERIOS/TERIOS_2006/9708/004-006-1000A_S000A_738TC_T00G0.pdf
- [25] ECOpoint Inc (2013). *Emission Test Cycles. EPA Urban Dynamometer Driving Schedule (UDDS) for Heavy-Duty Vehicles*. Retrieved September 23, 2013 from <http://www.dieselnets.com/standards/cycles/udds.php>
- [26] ECOpoint Inc (2013). *Emission Test Cycles. EPA Highway Fuel Economy Test Cycle (HWFET)*. Retrieved September 23, 2013 from <http://www.dieselnets.com/standards/cycles/udds.php>
- [27] Phantom Supercharger (2013). *Phantom Full Throttle Superchargers: TQ-25024V*. Retrieved October 3, 2013 from <http://www.phantomsuperchargers.com/fts-tq25024v.html>
- [28] CarLeasingMadeSimple.com (2013). *Perodua MYVI Kerb Weight*. Retrieved October 3, 2013 from <http://carleasingmadesimple.com/business-car-leasing/perodua/myvi/kerb-weight/>
- [29] Honda (2011). *Variable Cylinder Management (VCM) – iVTEC Accord V6*. Retrieved October 3, 2013 from <http://www.honda.co.nz/technology/emissions/vcm/>

APPENDICES

Appendix A – Specs & Compressor Map of Electric Supercharger [27]

<p><u>SPECIFICATIONS:</u></p> <p>Max airflow: ~400 CFM</p> <p>Supported engine power: up to 250 HP</p> <p>Typical base engine HP: 100-240</p> <p>Typical peak torque gain: 30-40%</p> <p>Pressure range: up to 1.3 PR</p> <p>Motor efficiency: ~90-94%</p> <p>Motor type: brushless w/ 3" leads</p>	<p>Compressor efficiency: 72-74%</p> <p>Lubrication: sealed ceramic bearings</p> <p>Weight: 4.0 lbs.</p> <p>Drive power: 3500 Watts</p> <p>Rating @ 20 C: 2 minutes (continuous)</p> <p>Rating @ 50 C: 1 minute (continuous)</p> <p>Maintenance: None</p>
---	--



Appendix B – Calculation of TDC Clearance Height

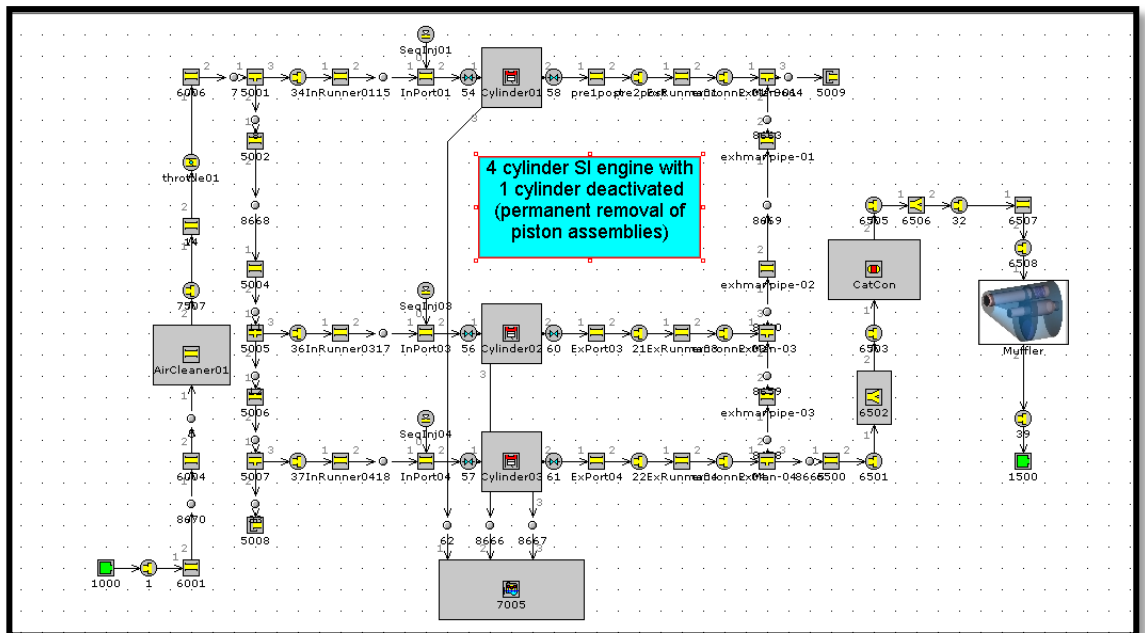
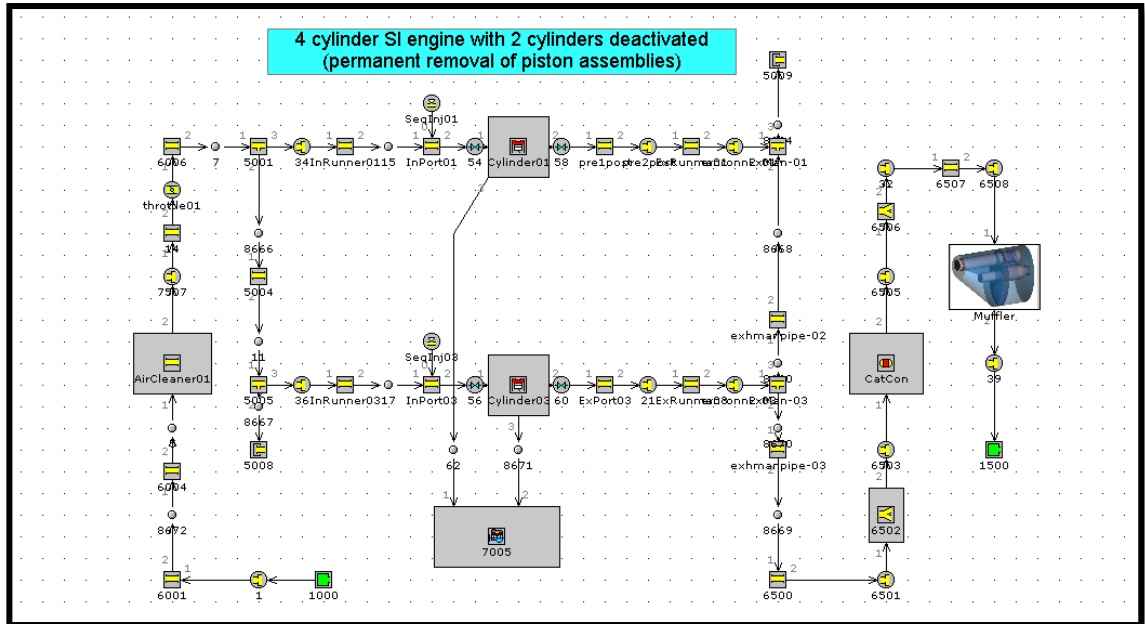
Compression Ratio, $r_c = \frac{V_h + V_c}{V_c}$

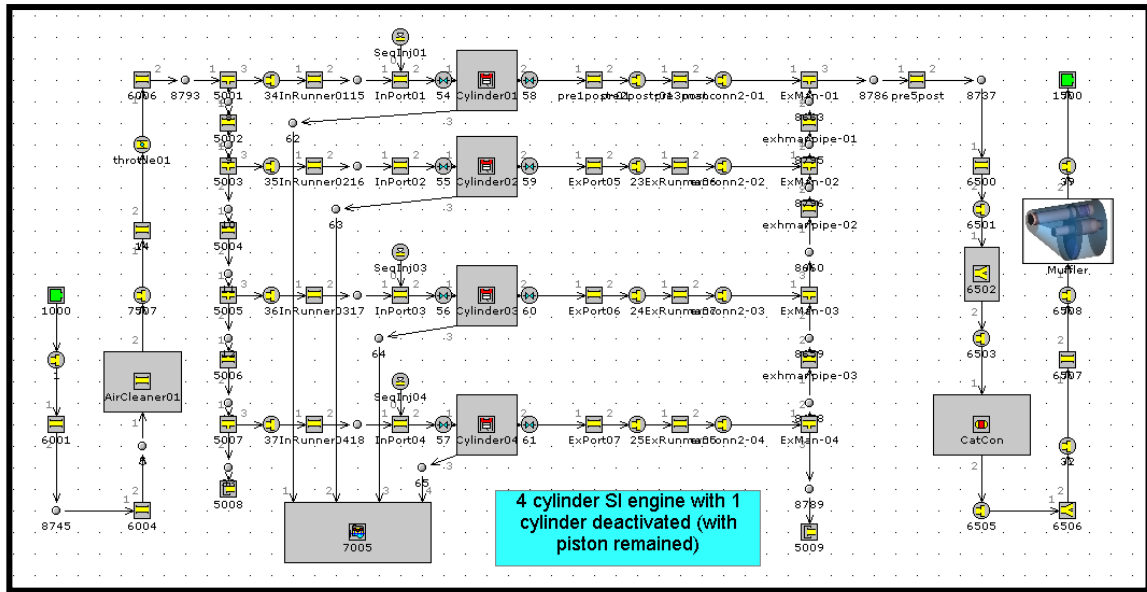
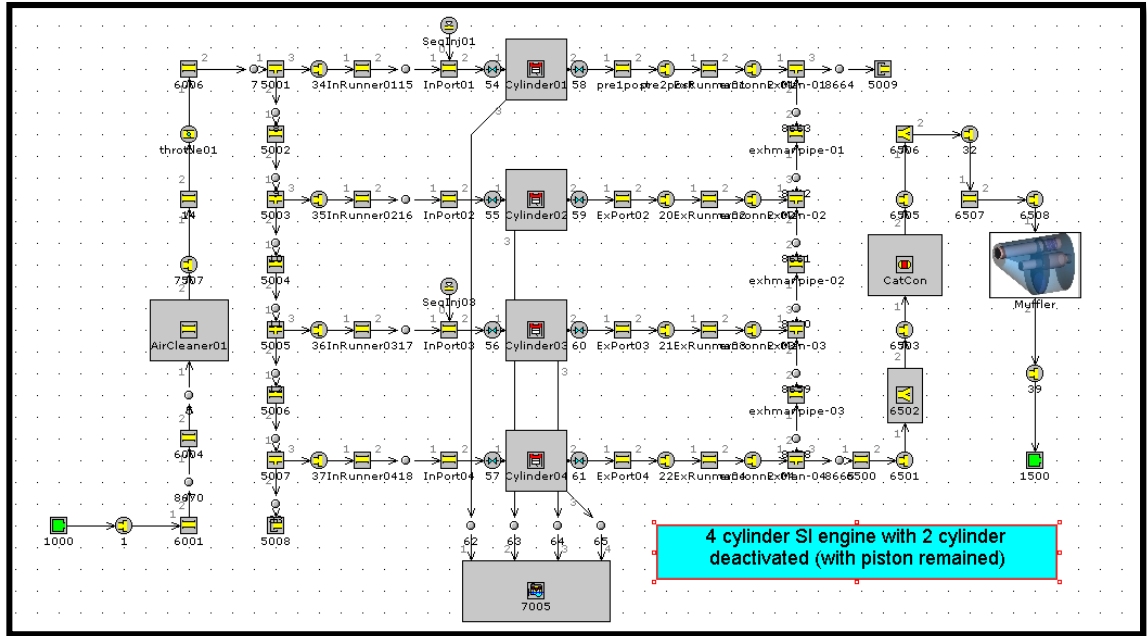
Cylinder displacement volume, $V_h = 1.3L/4 = 0.325L = 0.325 \cdot 10^6 \text{ mm}^3$

$9V_c = 0.325 \cdot 10^6 \text{ mm}^3 \rightarrow$ Clearance Volume, $V_c = 3.611 \cdot 10^5 \text{ mm}^3 = \pi B^2 h$

TDC Clearance Height, $h = \frac{V_c}{\pi B^2} = \frac{3.611 \cdot 10^5 \text{ mm}^3}{\pi (72 \text{ mm})^2} = 2.2 \text{ mm}$

Appendix C – Engine Map of Cylinder Deactivation Modules





Appendix D – Minimum Engine Power and Torque Required

The dynamic equation for a moving car up a slope will be;

$$M \frac{dv}{dt} = (F_{tf} + F_{tr}) - (F_{rf} + F_{rr} + F_w + F_g)$$

For front wheel drive ($F_{tr} = 0$),

$$M \frac{dv}{dt} = F_{tf} - (F_{rf} + F_{rr} + F_w + F_g)$$

Where

F_{tf} = Front Tractive Force

F_{rf} = Front Rolling Resistance Force

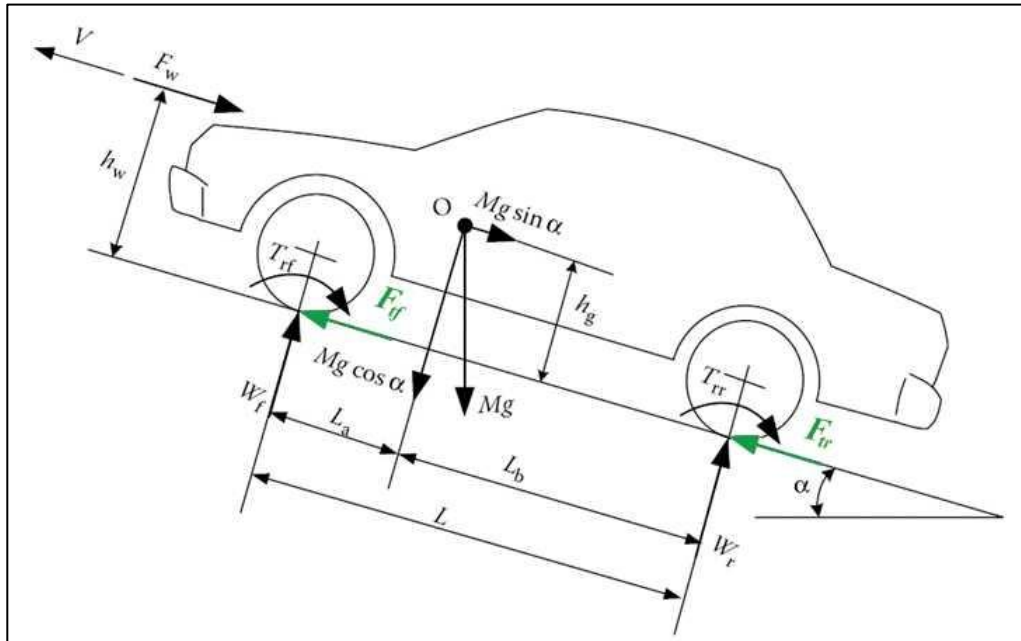
F_{rr} = Rear Rolling Resistance Force

F_{tr} = Rear Tractive Force

F_w = Aerodynamic Drag

$F_g = Mg \sin \alpha =$ Gradient/Climbing Resistance

Figure below illustrates the dynamic forces of the vehicle.



D-1 Constant Speed of 110km/h on Flat Asphalt Surface

Taking PERODUA Myvi 1.3 SX as the benchmarking model, all its physical parameters will be used in the calculation.

Rolling Resistance, $F_{rf} = F_{rr} = Pf_r \cos \alpha = \left(\frac{1}{2}M_T g\right) f_r \cos \alpha$

- Consider total mass is equal to the kerb mass of a Myvi car, in addition to the mass of four passengers (assumed 75kg each) [28],

$$M_T = M_{\text{car}} + M_{\text{ppl}} = 935\text{kg} + (45 \times 75\text{kg}) = 1310 \text{ kg};$$

- f_r , the rolling resistance coefficient, is taken as 0.013 for car tires on asphalt or concrete road;
- Angle of elevation of the slope is assumed to be 0° ;

$$F_{rf} = F_{rr} = \frac{1}{2}(1310 \text{ kg})(9.81 \text{ m/s}^2)(0.013) \cos 0^\circ = 83.53\text{N}$$

Aerodynamic Drag, $F_w = \frac{1}{2}\rho A_f C_D (V - V_w)^2$

Where,

ρ = density of air, taken as 1.2 kg/m³;

A_f = frontal area of car, with Myvi having a value of 2.19m² [29];

C_D = drag coefficient of the Myvi car, 0.35 based on experimented results [23];

V = speed of the car, desired at constant speed of 110km/h for = 30.56m/s;

V_w = speed of the wind, being neglected and valued as zero;

$$F_w = \frac{1}{2}\left(1.2 \frac{\text{kg}}{\text{m}^3}\right)(2.19\text{m}^2)(0.35)\left(30.56 \frac{\text{m}}{\text{s}}\right)^2 = 429.51\text{N}$$

Required Tractive Force, $F_{tf} = M \frac{dv}{dt} + (F_{rf} + F_{rr} + F_w + F_g)$

$$F_{tf} = 0N + (83.53N + 83.53N + 429.51N + 0N)$$

$$F_{tf} = F_t = 596.57N$$

Minimum Engine Power Required, $P = \frac{F_t V}{\eta_t}$

with η_t = efficiency of driveline assumed 100%

$$P = \frac{596.57N(30.56m/s)}{1} = 18231.2W = 18.2kW$$

Minimum Torque Output Required,

Assuming no slip of the tires,

$$F_{tf} = \frac{T_w}{r_d} = \frac{T_p i_g i_o \eta_t}{r_d} \rightarrow T_p = \frac{F_t r_d}{i_g i_o \eta_t}$$

where

i_g = gear ratio of transmission, using 4th gear at 110km/h = 0.865 [23];

i_o = gear ratio of the final drive, 4.267 for Myvi engine [23];

η_t = efficiency of driveline, assume 100%

r_d = radius of the wheel, taken as 583mm [23];

T_p = torque output

$$T_p = \frac{(596.57N)(0.583m)}{(0.865)(4.267)(1)} = 89.6N.m$$

D-2 Constant Speed of 30km/h up a Slope of 5.7°

Taking PERODUA Myvi 1.3 SX as the benchmarking model, all its physical parameters will be used in the calculation.

Rolling Resistance, $F_{rf} = F_{rr} = Pf_r \cos \alpha = \left(\frac{1}{2}M_T g\right) f_r \cos \alpha$

- Consider total mass is equal to the kerb mass of a Myvi car, in addition to the mass of four passengers (assumed 75kg each) [28],

$$M_T = M_{\text{car}} + M_{\text{ppl}} = 935\text{kg} + (5 \times 75\text{kg}) = 1310 \text{ kg};$$

- f_r , the rolling resistance coefficient, is taken as 0.013 for car tires on asphalt or concrete road;
- Angle of elevation of the slope is assumed to be a maximum of 5.7° from the flyover common standard of gradient 1:10;

$$F_{rf} = F_{rr} = \frac{1}{2}(1310 \text{ kg})(9.81 \text{ m/s}^2)(0.013) \cos 5.7^\circ = 83.12\text{N}$$

Aerodynamic Drag, $F_w = \frac{1}{2}\rho A_f C_D (V - V_w)^2$

Where,

ρ = density of air, taken as 1.2 kg/m³;

A_f = frontal area of car, with Myvi having a value of 2.19m² [29];

C_D = drag coefficient of the Myvi car, 0.35 based on experimented results [23];

V = speed of the car, desired at constant speed of 30km/h for = 8.33m/s;

V_w = speed of the wind, being neglected and valued as zero;

$$F_w = \frac{1}{2}\left(1.2 \frac{\text{kg}}{\text{m}^3}\right)(2.19\text{m}^2)(0.35)\left(8.33 \frac{\text{m}}{\text{s}}\right)^2 = 31.91\text{N}$$

Slope Climbing Resistance, $F_g = M_T g \sin \alpha$

$$F_g = (1310kg)(9.81m/s^2)\sin 5.7^\circ = 1276.4N;$$

Required Tractive Force, $F_{tf} = M \frac{dv}{dt} + (F_{rf} + F_{rr} + F_w + F_g)$

$$F_{tf} = 0N + (83.12N + 83.12N + 31.91N + 1276.4N)$$

$$F_{tf} = F_t = 1474.55N$$

Minimum Engine Power Required, $P = \frac{F_t V}{\eta_t}$

with η_t = efficiency of driveline assumed 100%

$$P = \frac{1474.55N(8.33m/s)}{1} = 12283W = 12.3kW$$

Minimum Torque Output Required,

Assuming no slip of the tires,

$$F_{tf} = \frac{T_w}{r_d} = \frac{T_p i_g i_o \eta_t}{r_d} \rightarrow T_p = \frac{F_t r_d}{i_g i_o \eta_t}$$

where

i_g = gear ratio of transmission, 1st gear up the slope = 3.182 [23];

i_o = gear ratio of the final drive, 4.267 for Myvi engine [23];

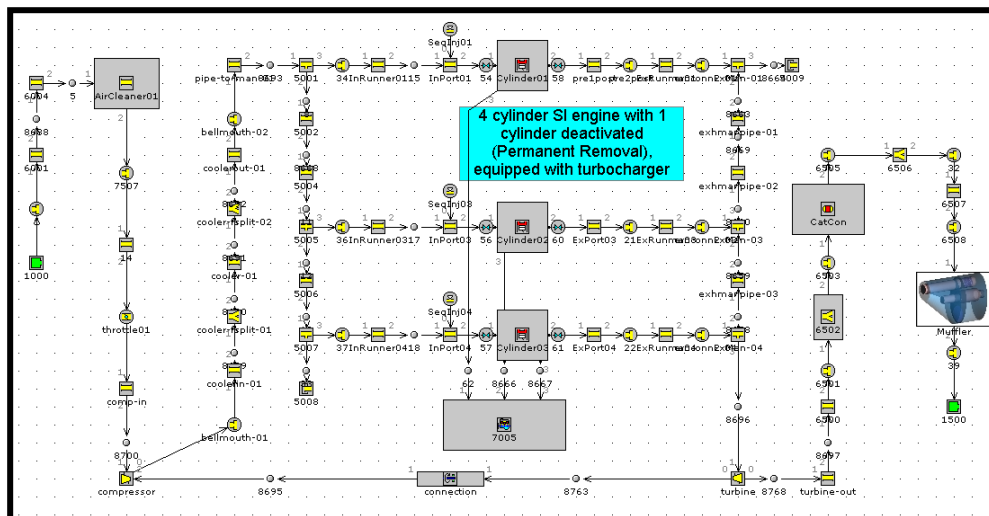
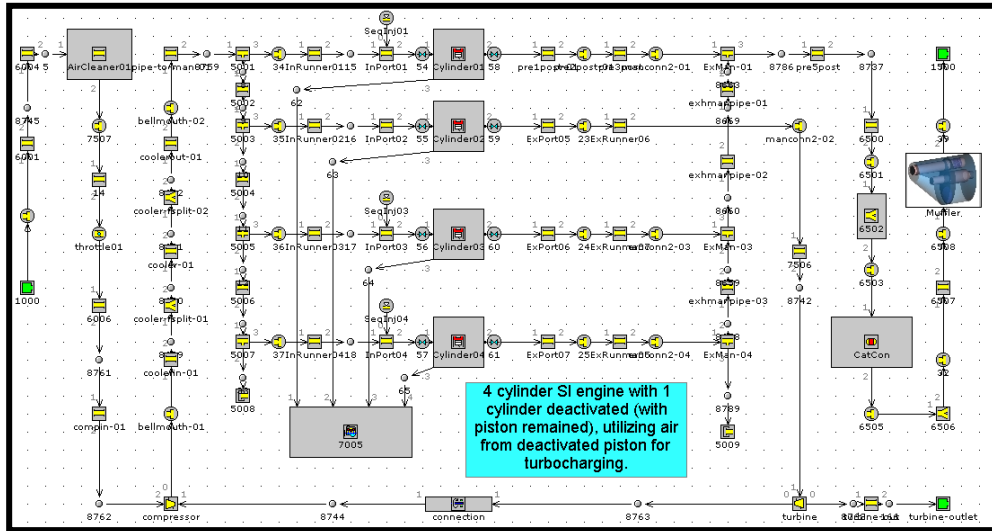
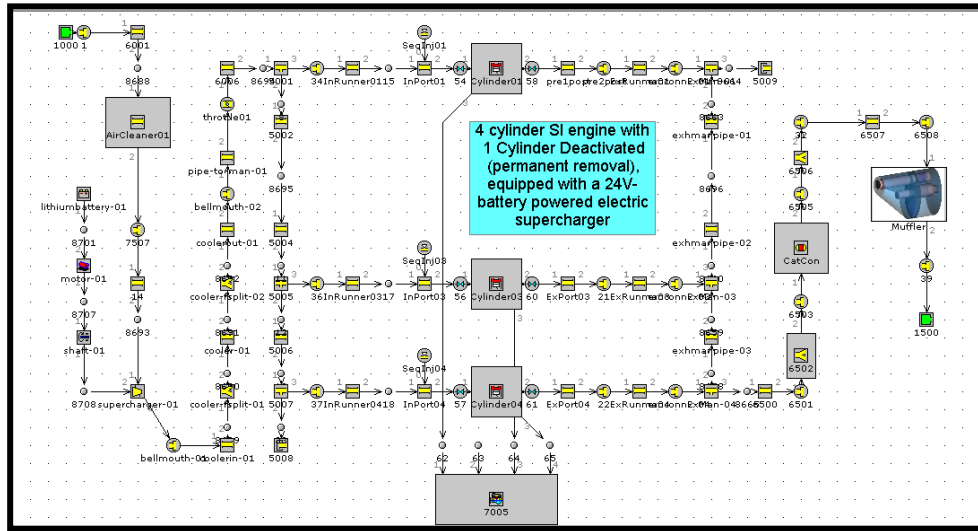
η_t = efficiency of driveline, assume 100%

r_d = radius of the wheel, taken as 583mm [23];

T_p = torque output

$$T_p = \frac{(1474.55N)(0.583m)}{(3.182)(4.267)(1)} = 63.3N.m$$

Appendix E – Engine Map of Forced Induction Modules



Appendix F – Driving Course of the Fuel Consumption Test



Red Route (Rounding UTP) – approximately 5.2km per round (drive 5 rounds) ;
Orange Route (to Petronas Petrol Station) – approximately 0.9 km ;
Pink Route (from Petronas Petrol Station) – approximately 0.8 km ;
Total = 27.7km

Appendix G – Vibrational Test

Although the previous ADAMS simulation section has simulated the vibration levels, an actual vibrational test had been carried out to support the statement that cylinder deactivation will increase the vibration forces drastically. The main purpose of the task aimed to know the vibration forces increment along with cylinder deactivation. By employing the PCB accelerometer with the NI LabVIEW software, the vibration level of the engine can be easily plotted and recorded.

The equipments were set up with three PCB accelerometers taped to three different axis; x, y, and z. The fuel injectors for Cylinder 1 & 3 are removed as in Figure G-1. The accelerometers were connected to the laptop running on NI LabVIEW software. A thermocouple has been used to detect the temperature on different surface area of the engine after the car engine was started for two minutes and recorded a temperature as high as 200°C. As a result, the accelerometers of upper temperature limit of only 98°C can only be taped on the air filter surface above the engine as shown in Figure G-1 below because the engine temperature might rise too high and damage the accelerometers. Anyhow the vibration forces of air filter will almost be perpendicular to those of engine.

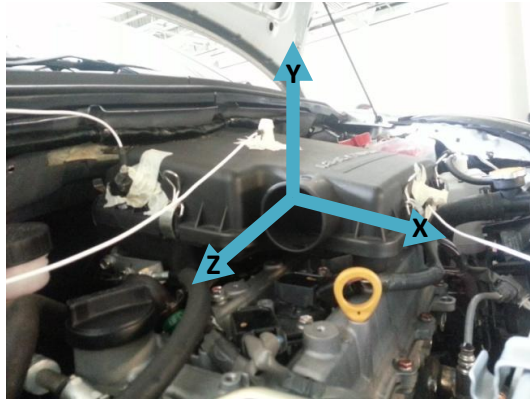
The vibration levels were recorded for three different axes;



(a) Accelerometers taped to Engine



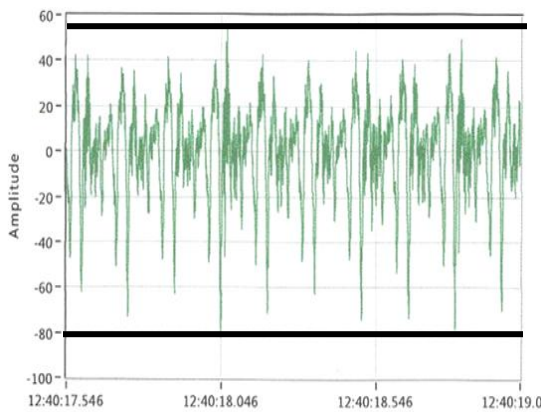
(b) Accelerometers connected to LabVIEW



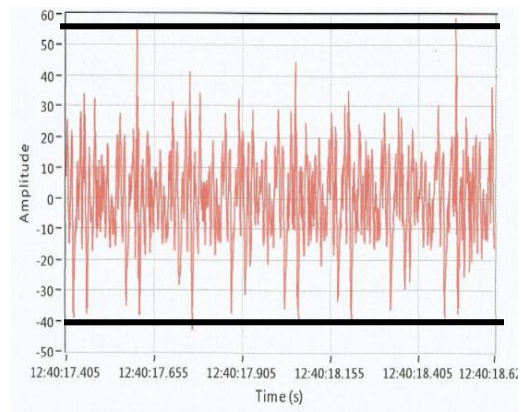
(c) Accelerometers connected in 3 different axis (d) Removal of Fuel Injectors

FIGURE G-1: Vibration Experiment Equipment Set Up

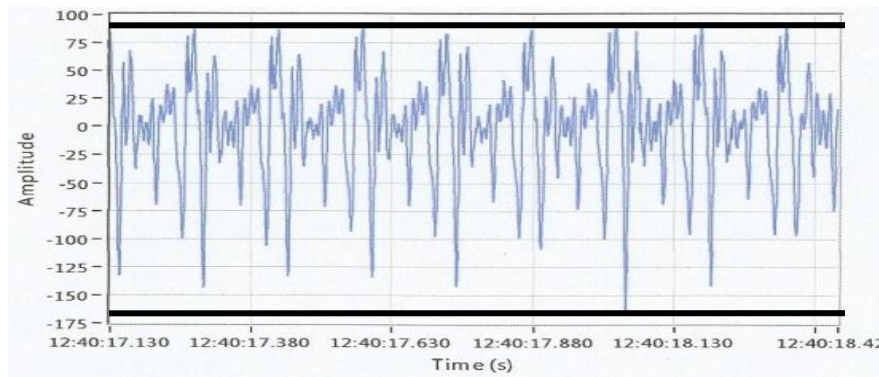
The car engine is started and run at 2000 rpm at neutral gear to check the vibrations and to compare between the vibration with and without deactivation of cylinder. The same is done for the deactivated engine. The results are as shown under Figure G-2 and G-3.;



(a) z-axis of amplitude -80N to 55N

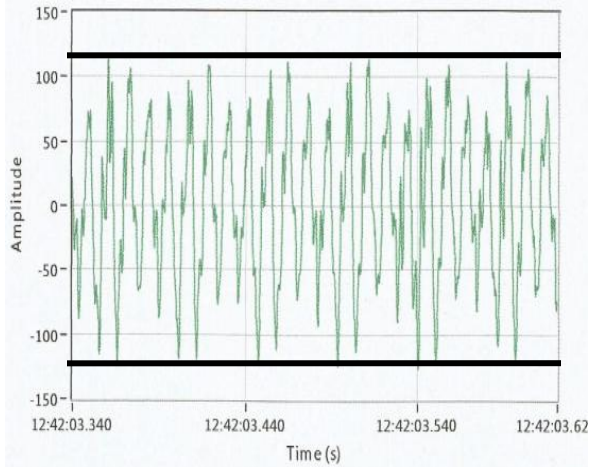


(b) x-axis of amplitude -40N to 55N

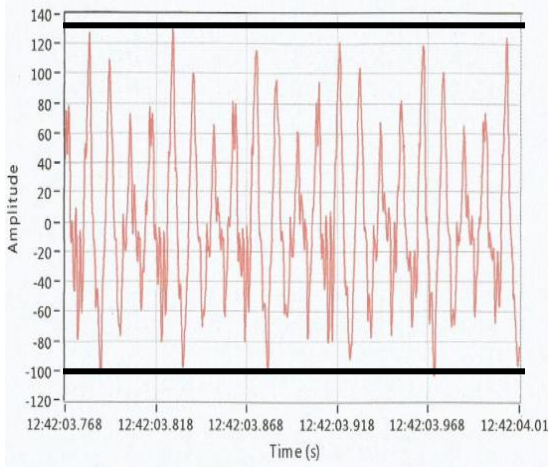


(c) y-axis of amplitude -170N to 90N

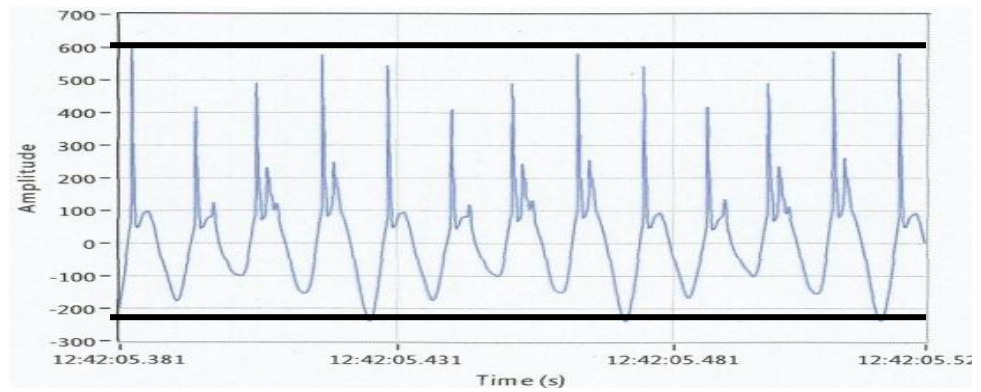
FIGURE G-2: Vibration Level of Normal Engine at 2000rpm



(a) z-axis of amplitude -125N to 115N



(b) x-axis of amplitude -100N to 130N



(c) y-axis of amplitude -220N to 600N

FIGURE G-3: Vibration Level of Deactivated Engine at 2000rpm

Appendix H – Resultant Moment along Crankshaft

As to calculate the resultant moment along the crankshaft, first the forces along the crankshaft have to be determined with their distance from the center of the crankshaft. The distances are determined from Figure H-1 while the vibration forces on crank pin 1, 2, 3 & 4 are all determined by subtracting the dynamic forces by the static forces as in Figure H-2. From CATIA model, $a = 92\text{mm}$, $a/2 = 46\text{mm}$, $3a/2 = 138\text{mm}$;

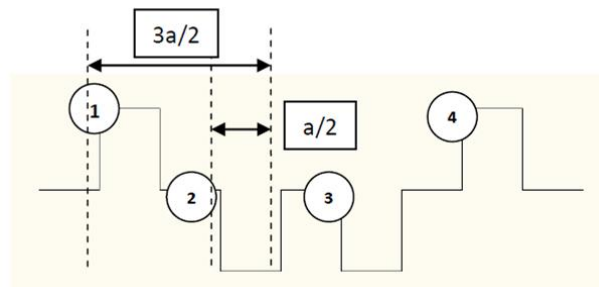


FIGURE H-1: Crank Throw Arrangement for Moment Calculation

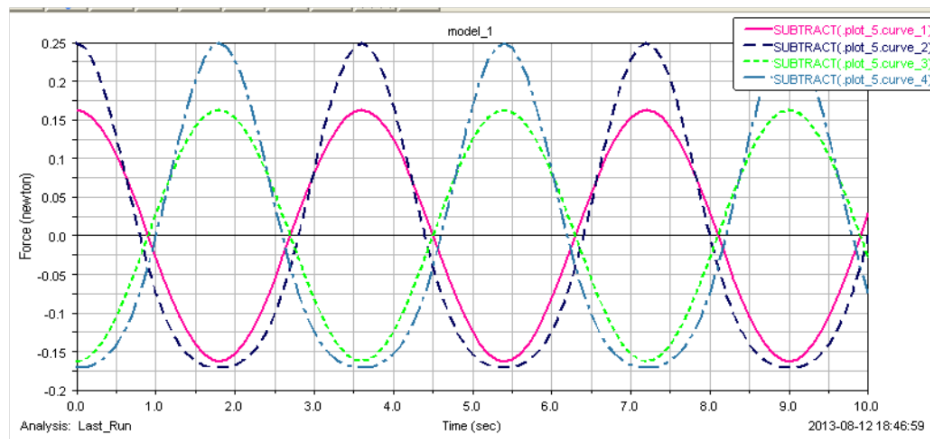


FIGURE H-2: Magnitude of Vibration of Each Crank Pin (Steel Balancer)

To get the graph for the moment, the graph of forces are scaled up or down with their distances from the center, achieving graphs in Figure H-3 after Graphs for piston 1 & 4 are scaled with 0.138 as in 0.138m while force graphs of piston 2 & 3 are multiplied by 0.046 as in 0.046m.

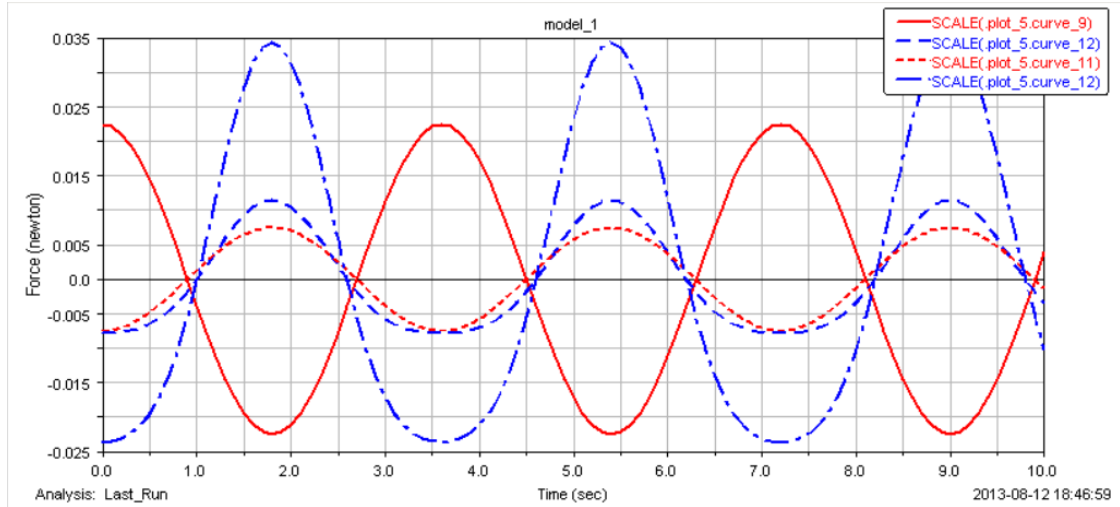


FIGURE H-3: Magnitude of Moment of Each Crank Pin (Without Steel Balancer)

Last but not least, all the moments of each crank pin are summed up together to get the overall resultant moment as in figure below.

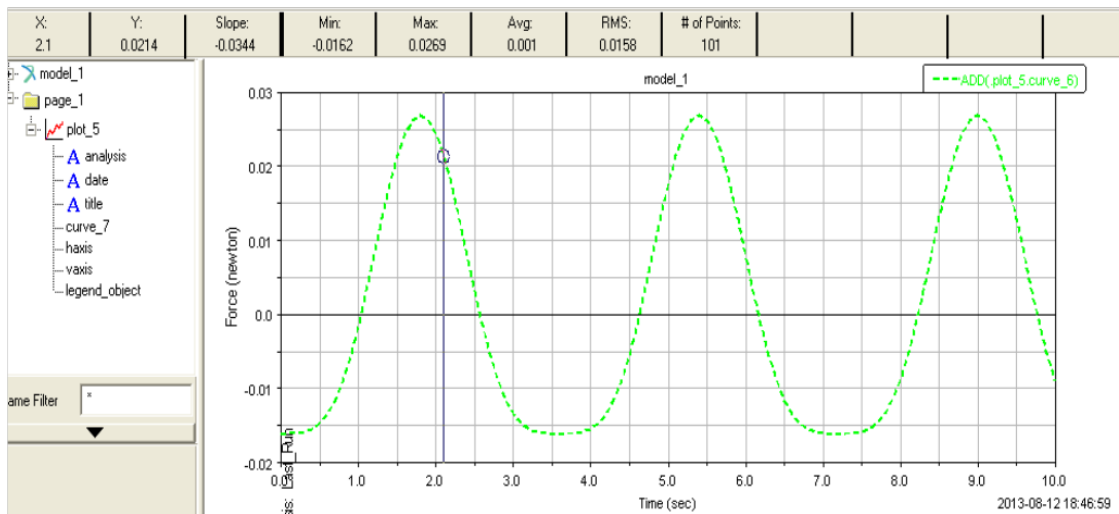


FIGURE H-3: Resultant Moment of Crankshaft (Without Steel Balancer)

The same steps are done for the crankshaft without steel balancers for cylinder deactivation.